Doctoral Dissertation (Censored)

博士論文 (要約)

Development of a method for large scale production of pancreatic islet progenitors derived from human iPS cells

(iPS 細胞由来膵前駆細胞の大量培養に向けた

膵前駆細胞増幅法の開発)

A Dissertation Submitted for the Degree of Doctor of Philosophy

January 2020

令和 2 年　1 月博士（理学）申請

Department of Biological Sciences, Graduate School of Science,

The University of Tokyo

東京大学大学院理学系研究科

生物科学専攻

Anna Tanaka

田中 杏奈

Table of Contents

List of Abbreviations

2-ME: 2-mercaptoethanol (2-ME)

2D: 2 dimensional

3D: 3 dimensional

Arx: Aristaless related homeobox

BMI1: B lymphoma Mo-MLV insertion region 1 homolog

c-Kit: KIT proto-oncogene receptor tyrosine kinase

c-MYC: MYC proto-oncogene, bHLH transcription factor

C-peptide: Connecting peptide

CD: Cluster of differentiation

CDKs: Cyclin dependent kinases

CXCR4: C-X-C chemokine receptor type 4

Cdkn1a: Cyclin-dependent kinase inhibitor 1

DAPI : 4'-6-diamidino-2-phenylindole

DE: Definitive endoderm

DMEM: Dulbecco's Modified Eagle's Medium

E: Embryonic day

EF1α: Elongation factor 1 alpha 1

EGF: Epidermal growth factor

EP: Endocrine progenitor

Ex4: Exendin-4

FACS: Fluorescence activated cell sorting

FGF: Fibroblast growth factor

G1 phase: Gap 1 phase

GAPDH: Glyceraldehyde-3-phosphate dehydrogenase

GCG: Glucagon

GFP: Green fluorescent protein

GSIS: Glucose-stimulated insulin secretion

HEK293: Human embryonic kidney cells 293

hESCs: Human embryonic stem cells

hiPSCs: Human induced pluripotent stem cells

hPSC: Human pluripotent stem cells

hTERT: Human telomerase reverse transcriptase

IGF: Insulin-like growth factor

INS: Insulin

KRBH: Krebs-Ringer bicarbonate-HEPES buffer

Ki67: Marker of proliferation Ki-67

LV-Cre: Cre expressing lentivirus

MAFA: MAF bZIP transcription factor A

MOI: Multiplicity of infection

NEAA: MEM Non-Essential Amino Acids

NEUROD1: Neuronal differentiation 1

NGN3: Neurogenin3

NKX2.2: NK2 homeobox 2

NKX6.1: NK6 homeobox 1

PAX4: Paired box 4

PAX6: Paired box 6

PBS: Phosphate-buffered saline

RPMI: Roswell Park Memorial Institute media

PEI: Polyethylenimine

PP: Pancreatic progenitor

PSG: Penicillin Streptomycin Glutamine

Pdx1: Pancreatic and duodenal homeobox 1

Ptf1a: Pancreas associated transcription factor 1a

qRT-PCR: Quantitative real-time polymerase chain reaction

RB: Retinoblastoma

SD: Standard deviation

SIX3: SIX homeobox 3

SOX9: SRY-box transcription factor 9

SST: Somatostatin

SUSD2: Sushi domain containing 2

SV40LT: Simian virus-40 large T-antigen

UCN3: Urocortin 3

Abstract

Transplantation of pancreatic islets is an effective therapy for severe type 1 diabetes. As donor shortage is a major problem for this therapy, attempts have been made to produce a large number of pancreatic islets from human pluripotent stem cells (hPSCs). However, as the differentiation of hPSCs to pancreatic islets requires multiple and lengthy processes using various expensive cytokines, the process is variable and low efficiency and costly. Therefore, it would be beneficial if islet progenitors could be expanded while maintaining their differentiation potential, and the aim of this study was to test this possibility in an in vitro differentiation protocol for pancreatic islets from human induced pluripotent stem cells (hiPSCs). Taking advantage of a modified hiPSC line with a genetically encoded fluorescent marker, Neurogenin3 (NGN3)-expressing pancreatic endocrine progenitor (EP) cells derived from hiPSCs were isolated. While they exhibited the ability to differentiate into pancreatic islets, their cell cycle was arrested. By using a lentivirus vector, I introduced several growth promoting genes into the NGN3-expressing EP cells. I found that Simian virus-40 large T-antigen (SV40LT) expression induced proliferation of the cells but reduced the expression of endocrine-lineage commitment factors, *NGN3*, *NEUROD1*, and *NKX2.2*, resulting in the suppression of islet differentiation. Removing

SV40LT by using the Cre-loxP system after the expansion led to the re-expression of endocrine-lineage commitment genes and restored the cells' ability to differentiate into functional islets. Thus, the present study will lead to a way to generate a large quantity of functional pancreatic islets through the expansion of EP cells from hPSCs.

Introduction

1. Structure, function, and development of the pancreas

The pancreas consists of exocrine and endocrine cells, which produce digestive enzymes and hormones, respectively, and is a key organ for digestion and blood glucose regulation. It is composed of 90% of exocrine cells and 10% of pancreatic ducts and endocrine cells (Figure 1A, 1B). The exocrine acinar structure is formed of several pyramidal-shaped acinar cells and lobules are formed by several acini. Acinar cells secrete digestive enzymes such as amylase and lipase by the stimulation of cholecystokinin and/or secretin from gastrointestinal enteroendocrine cells. The digestive enzymes secreted from the acinar cells pass through the acinar-connected distal duct, consisting of centroacinar cells and terminal ducts. These ducts connect to proximal ducts, which consist of the interlobular and main ducts that flow digestive enzymes into the duodenum (Figure 1A). Pancreatic islets are the intrapancreatic tissue composed of several endocrine cells such as α cells, β cells, and δ cells that play an essential role in the control of blood glucose levels (Figure 1C). Especially, pancreatic β cells secrete insulin, the only hormone that controls glycemia in response to blood glucose levels. On the other hand, α cells secrete glucagon that increases blood glucose levels, δ cells secrete

somatostatin that suppresses the secretion of insulin and glucagon. In pancreatic islets, a microvascular network is developed and plays a role for flowing blood glucose to islets and transporting various hormones secreted by pancreatic islet cells to the blood (Figure 1C) (Konstantinova & Lammert, 2004). These endocrine cells interact with each other in response to the blood glucose levels, resulting in strict control of the secretion of hormones (Jain & Lammert, 2009). Impaired control of the hormone secretion has a significant impact on homeostasis.

In mouse development, dorsal and ventral pancreatic buds arise from the primitive foregut tube at approximately embryonic day (E) 8.5. From E9.5 to E12.5, $Pdx1^{+}/Ptf1a^{+}/Nkx6.1^{+}$ multipotent pancreatic progenitor (PP) cells expand in each pancreatic bud. After approximately E13.5, each pancreatic bud forms a branching structure and is compartmentalized into the $Ptf1a^{+}$ tip and $Nkx6.1^{+}$ trunk region. At around E14.5, the ventral pancreatic bud rotates to dorsally, and these buds fuse to form one pancreas (Figure 2A) (Benitez et al., 2012). As development proceeds, the $Ptf1a^{+}$ tip region differentiates and forms the exocrine acinar structure, including the distal pancreatic duct. On the other hand, the $Nkx6.1^{+}$ trunk region mainly becomes the proximal pancreatic duct structure, and some cells differentiate and form endocrine cell cluster islet of Langerhans (Figure 2B) (Schaffer et al., 2010).

2. Transcription factors for pancreatic development

Pdx1 is a key transcription factor of pancreatic cell-fate commitment, and *Pdx1*-deficient mice lack the pancreas (Offield et al., 1996). Moreover, cell lineage tracing has shown that all pancreatic epithelial cells are derived from Pdx1-lineage cells (Gu et al., 2002). In adult mice, Pdx1 deletion in mature β cells resulted in cellular dysfunction and severe hyperglycemia (Gao et al., 2014).

Ptf1a is another transcription factor that is essential for pancreatic development. Expression of Ptf1a is restricted in pancreatic buds at the foregut endoderm and these lineage cells differentiate into all pancreatic epithelial cell types, exocrine, endocrine, and pancreatic ducts. Lack of Ptf1a results in the conversion of the PP cells into duodenum cells (Kawaguchi et al., 2002). At a later stage in pancreas development, it plays an essential role in exocrine function of acinar cells. In adult mice, Ptf1a-deletion in acinar cells also induces cell dysfunction and result in acinar to ductal metaplasia (Krah et al., 2015).

Nkx6.1 is an important transcriptional factor for early stage of pancreas development and generation of β cell lineage (Sander et al., 2000). Pancreas-specific Nkx6.1 deletion leads to decrease in the Neurogenin-3 (Ngn3)-expressing EP cells at approximately E14.5

in mice (Schaffer et al., 2010), and the β cell specific ablation of Nkx6.1 results in dysfunction of insulin biosynthesis and secretion in pancreatic β cells (Taylor et al., 2013).

Ngn3 is a master regulator for EP cells, and pancreatic endocrine cells disappeared in Ngn3 knockout mice (Gradwohl et al., 2000). In the mouse pancreas development, some epithelial cells in the Nkx6.1-expressing trunk region express Ngn3 at a high level and become EP cells. Ngn3 directly induces the expression of NeuroD1 and Nkx2.2, which are essential for endocrine cell differentiation and function, especially β cells (Naya et al., 1997)(Sussel et al., 1998). It has been reported that many transcription factors such as Nkx2.2, Nkx6.1, Pax4, MafA are important for the fate determination of β cells and their function, while Pax6 and Arx are important for determining the α cell fate (Collombat et al., 2003).

3. Diabetes and therapy

Diabetes is a chronic metabolic disease characterized by elevated levels of blood glucose, which leads to serious damage to the heart, blood vessels, eyes, kidneys, and nerves (Ashcroft & Rorsman, 2012). There are two types of diabetes, type 1 and type 2 diabetes. Type 1 diabetes is a disorder caused by the autoimmune destruction of insulin-producing pancreatic β cells, resulting in a shortage of insulin (Mathis et al.,

2001)(Gallagher et al., 2015). Patients of type 1 diabetes need a daily injection of insulin, but insulin injection alone cannot properly control glycemia in severe cases. In contrast, type 2 diabetes is characterized by insulin insufficiency or insulin resistance. Dietary restriction and routine exercise are effective for some patients of type 2 diabetes. In severe cases, patients need a medication therapy, such as suppression of glucose production, stimulation of insulin secretion, enhancing insulin sensitivity, and so on. While many drugs have been developed for type 2 diabetes, lifelong use of the drugs often causes side effects. Diabetic patients of both type 1 and type 2 are increasing worldwide, being a major social problem.

For severe insulin-dependent patients whose blood glucose levels cannot be controlled by insulin injection, transplantation of pancreas or pancreatic islet is the only effective treatment (Shapiro et al., 2000). Pancreatic islets isolated from cadaveric donors or brain-dead donors are transplanted into the liver via the portal vein, which is less invasive than pancreas transplantation. However, a serious donor shortage and immune rejection are major bottlenecks to spread this treatment worldwide (Shapiro et al., 2006). In order to solve the donor shortage, significant efforts have been made to differentiate pancreatic β cells or islets from human pluripotent stem cells (hPSCs) with a potential to proliferate

indefinitely, such as embryonic stem cells (hESCs) and induced pluripotent stem cells (hiPSCs) (Zhou & Melton, 2018).

4. Generation of functional pancreatic β cells from PSCs

Pancreatic β cells derived from hESCs / hiPSCs are an attractive cell source for a new therapy of type 1 diabetes. There are many reports showing the generation of insulin secreting pancreatic β cells from hESCs / hiPSCs since 2000 (Soria et al., 2000). Based on pancreatic development, a differentiation method of hESCs was established in 2006 (D'Amour et al., 2006). It was shown that human pancreatic endocrine cells were generated *via* multiple steps similar to pancreatic development in fetus, i.e. definitive endoderm (DE), posterior foregut tube (PFG), PP cells, EP cells, and finally hormone-producing endocrine cells including β cells. However, insulin secretion from the β cells produced by this method was clearly insufficient compared with that *in vivo*. Therefore, the same research group changed its strategy and tried to transplant EP cells into mouse epididymal adipose tissue for maturation *in vivo* (Kroon et al., 2008). As a result, mature β cells secreting human insulin were successfully developed. While their strategy may provide a novel means for cell therapy of diabetes, their study indicated the difficulty of producing mature β cells *in vitro*.

Since then, significant efforts have been made to improve the protocol to generate mature β cells *in vitro* from PSCs by searching for effective cytokines and culture methods. Recently, several groups including ours have established protocols to generate β cells with the ability to secrete insulin in response to high glucose concentration. Furthermore, transplantation of those β cells in diabetic mice normalized the blood glucose levels (Data not shown)(Pagliuca et al., 2014)(Rezania et al., 2014)(Russ et al., 2015) (Yabe et al., 2019). Further, more detailed characteristics of differentiated cells are being identified by single cell RNA sequencing (Veres et al., 2019). A recent study revealed that PSC-derived β cells were different from the native pancreatic β cells; for example, the expression levels of UCN3, MAFA, and SIX3 were low in PSC-derived β cells.

While clinical trials are in progress or going to start by using immature pancreatic progenitors or β cells derived from hESCs / hiPSCs (Senior & Pettus, 2019), clinical application requires a large number of β cells and hence there are two major problems with the stepwise differentiation methods. First, as the differentiation efficiencies of the EP cells and hormone-producing endocrine cells are low and variable, it is difficult to reproducibly produce a large number of β cells or islets from hiPSCs. Second, as cytokines and media used for the differentiation are expensive (Kondo et al., 2018), the costs to produce islets *in vitro* are huge and should be significantly reduced. For clinical

use of those cells, it is necessary to establish a culture method to produce functional islets or β cells from hPSCs at a low cost in a large scale.

5. Toward a large scale production of islets from hiPSCs

Although PSCs proliferate indefinitely, their proliferation potential declines along the differentiation to mature cells. If one needs 100 million mature cells for therapy, 100 million PSCs are required at the beginning of differentiation even if 100% of PSC become the mature cells. In order to produce a large quantity of islets at a reasonable cost, it would be beneficial if islet progenitors can be expanded. Previous reports showed expansion of the cells at the early stage or middle stage of differentiation to pancreatic β cells, DE or PP cells (Sneddon et al., 2012)(Kimura et al., 2017). However, differentiation efficiency was notably reduced after the PP stage in the stepwise β cell differentiation protocol (Sharon et al., 2019)(Nair et al., 2019). Therefore, expanding islet progenitor cells at the EP stage should be more effective for mass production of hiPSC-derived islets, while there has been no such study aiming to expand EP cells.

For the control of blood glucose levels, it is important to generate not only β cells but also the other endocrine cell types of the islet, including glucagon-producing α cells that enhance the β cells function (Kojima et al., 2014)(Traub et al., 2017). Because all the

endocrine cell types arise from NGN3-expressing EP cells (Zhu et al., 2016)(Liu et al., 2014), it would be ideal if EP cells could be expanded and induced to differentiate to functional islets. In this present study, I have attempted to establish a method to expand NGN3-expressing EP cells and generate functional pancreatic islets.

Materials and Methods

Cell culture and differentiation

The hiPSC line hIveNry was described previously (Yamashita-Sugahara et al., 2016). hiPSCs were maintained and passaged in StemFlex Medium (Thermo Fisher Scientific, Waltham, MA). Cultured hiPSCs were seeded at 2×10^6 cells/cm^2 on six-well plates coated with Matrigel hESC-qualified Matrix (Corning, Corning, NY) in StemFlex Medium with 10 μM Y-27632 (Tokyo Chemical Industry, Tokyo, Japan) at 2 days before induction of differentiation, and medium was changed the next day to D-MEM/Ham's F-12 medium (D-MEM/F-12 medium) (FUJIFILM Wako Pure Chemical Corp, Osaka, Japan) with 20% Knockout Serum Replacement for ESCs/iPSCs (Gibco, Grand Island, NY), 1 × MEM Non-Essential Amino Acids (NEAA) (Gibco), 1 × Penicillin Streptomycin Glutamine (PSG) (Gibco), 55 μM 2-mercaptoethanol (2-ME) (Gibco), and 0.15 μM Stauprimide (Cayman Chemical Company, Ann Arbor, MI) for 1 day. The next day, differentiation was induced to pancreatic islets.

Pancreatic islets differentiation from hiPSCs.

Differentiation into pancreatic islets was conducted as described (Yabe et al., 2019) with the following modification.

Day 1: Roswell Park Memorial Institute media (RPMI)-1640 Medium (Sigma-Aldrich, St. Louis, MO) supplemented with 1 × non-essential amino acids (NEAA) (Gibco, Grand Island, NY), 1 × Penicillin Streptomycin Glutamine (PSG) (Gibco), 1 mM Sodium Pyruvate Solution (SP) (FUJIFILM Wako Pure Chemical Corp., Osaka, Japan), 55 μM 2-mercaptoethanol (2-ME) (Gibco), 100 ng/ml recombinant human activin A (Peprotech, Rocky Hill, NJ), and 3 mM CHIR99021 (FUJIFILM Wako Pure Chemical Corp).

Day 2: RPMI-1640 Medium supplemented with 1 × NEAA, 1 × PSG, 1 mM SP, 55 μM 2-ME, and 100 ng/ml recombinant human activin A.

Day 3-4: RPMI-1640 Medium supplemented with 1× B27 supplement (Gibco), 1 × NEAA, 1 × PSG, 1 mM SP, 55 μM 2-ME, and 100 ng/ml recombinant human activin A.

Day 5-7: Dulbecco's Modified Eagle's Medium – high glucose (DMEM medium) (Sigma-Aldrich) further supplemented with 1× B27 supplement, 1× NEAA, 1× PSG, 10 μM SB431542 (Tokyo Chemical Industry, Tokyo, Japan), 50 ng/mL recombinant human fibroblast growth factor (FGF) 10 (Peprotech), 0.25 μM SANT-1 (Cayman Chemical Company, Ann Arbor, MI), 1 μM Dorsomorphin (Tokyo Chemical Industry),

300 nM Indolactam V (Cayman Chemical Company), and 700 nM EC23 (reinnervate, Sedgefield, UK).

Day 8-12: DMEM medium further supplemented with 1 × B27 supplement, 1 × NEAA, 1 × PSG, 10 μM SB431542, 0.25 μM SANT1, 1 μM Dorsomorphin, 300 nmol/L Indolactam V, 700 nM EC23, 2.5 μM Repsox (BioVision, Milpitas, CA), and 5 μM $ZnSO_4$ (Sigma-Aldrich).

Day 13-20 (Stage 4 medium): DMEM medium further supplemented with 1 × B27 supplement, 1 × NEAA, 1 × PSG, 0.25 μM SANT-1, 1 μM Dorsomorphin, 10 μM DAPT (Tokyo Chemical Industry), 5 μM Repsox, 50 ng/mL insulin-like growth factor (IGF) (Peprotech), 50 ng/mL Exendin-4 (Ex-4) (abcam, Cambridge, United Kingdom), 20 ng/mL recombinant human epidermal growth factor (EGF) (Peprotech), 10 μg/mL Heparin (Sigma-Aldrich), 5 μM $ZnSO_4$, and 5 mM Nicotinamide (FUJIFILM Wako Pure Chemical Corp).

Day 21-30 (Stage 5 medium): D-MEM/F-12 medium further supplemented with 1 × B27 supplement, 1 × NEAA, 1 × PSG, 0.5 mM HEPES (Gibco), 2.5 μM Repsox, 50 ng/mL IGF, 50 ng/mL Ex-4, 50 ng/mL Glucagon-like Peptide 1 (Peptide institute, Osaka, Japan), 2 mM Nicotinamide, 10 μM forskolin (FUJIFILM Wako Pure Chemical Corp), 0.25 μM SANT-1, and 55 μM 2-ME.

From day 1 to day 20, cells were culture in 2D adherent conditions. At day 21, cells were dissociated into single cells and were suspended in Stage 5 medium with 10 μM Y-27632. The cell suspension was subjected to a 3D suspension culture condition in six-well plates, and the culture was continued from day 21 to day 30.

Lentivirus production

Lentivirus production was performed as described (Sakaue-Sawano et al., 2008)(Jiang et al., 2015). By using the lentiviral vector pCSII-EF-mKO2-hCdt1 (Sakaue-Sawano et al., 2008), we inserted TurboGFP, SV40LT, hTERT, c-MYC, BMI1, and Cre under the control of the EF1α promoter. TurboGFP, SV40LT, hTERT, c-MYC, BMI1, and Cre were derived from pCW57-MCS1-P2A-MCS2 (GFP) (Addgene, #80924), pEP4 E02S ET2K (Addgene, #20927), pCDH-3×FLAG-TERT (Addgene, #51631), pCDH-puro-cMyc (Addgene, #46970), pT3-EF1α-Bmi1 (Addgene, #31783), and pCAGGS-Cre (RIKEN BRC DNA BANK), respectively. Furthermore, we generated pCSII-EF-SV40LT-IRES-mCD2-loxP, in which SV40LT was flanked by the loxP sequences. The mouse CD2 (mCD2) cDNA was cloned from the mouse spleen. HEK293FT cells were transfected with three plasmids: packaging plasmid (pCAG-HIVgp, RIKEN), envelop plasmid (pCMV-VSV-G-RSV-Rev, RIKEN), and the SIN vector plasmid using the

polyethylenimine (PEI) “max” (Polysciences, Warrington, PA) transfection. Viral titers were determined by infection of HEK293T cells with serial dilutions of the viral stocks, followed by flow cytometric analysis for a fluorescent protein or antibody.

Lentivirus Transduction

Lentivirus transduction was performed using ViroMag R/L (OZ Bioscience, Marseille, France) according to the manufacture’s protocol. *NGN3*-mCherry^{high} cells were transduced with a lentivirus at a MOI of 2 for 24 hours by using ViroMag R/L.

Expansion culture of *NGN3*-mCherry^{high} cells

Forty-eight hours after lentivirus transduction, *NGN3*-mCherry^{high} cells were dissociated into single cells using 1 × TrypLE^{TM} Select Enzyme (TrypLE) (Gibco). After dissociating to a single cell with TrypLE, the number of cells was counted using a hemocytometer. Trypan blue dye was used to determine the viability of cells, and there were almost no positive cells at each passage. *NGN3*-mCherry^{high} cells were suspended in Stage 4 medium with 10 μM Y-27632 and the cell suspension was cultured in a six-well plate. From the next day, Stage 4 medium without Y-27632 was used.

Flow cytometric analysis of cytoplasmic and nuclear proteins

Intracellular staining was performed using the Transcription factor buffer kit (BD Biosciences, San Jose, CA) according to the manufacture's protocol. Antibodies used are listed in Tables 1 and 2.

Quantitative RT-PCR

Total RNA was extracted using TRIzol reagent (Invitrogen Life Technologies, Carlsbad, CA) according to the manufacture's protocol. Residual genomic DNA was digested with DNase I (Invitrogen Life Technologies). First-strand cDNA was synthesized using PrimeScriptII 1st strand cDNA Synthesis Kit (Takara Bio, Shiga, Japan). Quantitative RT-PCR was performed using SYBR Premix EX TaqII (Takara Bio). All data were calculated using the ddCt method with *GAPDH* as a normalization control. Primers used are listed in Table 3.

C-peptide release assay.

hiPSC-derived islets were washed 3 times with Krebs-Ringer bicarbonate-HEPES buffer (KRBH) and pre-incubated with KRBH for 2 hours. The cells were then incubated with KRBH containing 2.5 mM glucose for 30 minutes. After washing 3 times with

KRBH the cells were incubated with 2.5 mM glucose in KRBH buffer for 1 hour and the supernatant was collected. Next, the cells were incubated with 25 mM glucose in KRBH buffer for 1 hour and the supernatant was collected. After glucose challenge test, the number of cells was counted using a hemocytometer. Insulin secretion in the supernatants was evaluated by using a Human Ultrasensitive C-peptide ELISA kit (Mercodia, Uppsala, Sweden).

Immunocytofluorescence

Immunocytofluorescence was carried out as previously described (Nakano et al., 2015). Briefly, hiPSC-derived islets were fixed in 4% paraformaldehyde on ice for 20 minutes. The cells were blocked with 5% skim milk (BD Biosciences) for 30 minutes and incubated with primary antibodies (Table 1) at 4˚C overnight. After washing three times with PBS, cells were incubated with fluorescence-conjugated secondary antibodies (Table 2) and 4'-6-diamidino-2-phenylindole (DAPI) for nuclear stain.

Statistical analysis

Values are expressed as mean ± SD. Statistical analyses were performed using either Student’s t test or the Mann-Whitney U test to evaluate differences between groups. A

comparison of gene expression in multiple fractions was done using the Tukey-Kramer test. A p value less than 0.05 was considered statistically significant for all analyses.

Results

Differentiation of endocrine progenitor (EP) from hiPSCs

hiPSCs were differentiated into EP cells by the stepwise protocol following the developmental process (Yabe et al., 2017) with some modification as described in Materials & Methods and Figure 3. The differentiation efficiency in each stage was evaluated by expression of cell specific marker(s) (Figure 4). At the DE stage, CXCR4- and c-Kit-expressing cells were 85.79 ± 6.28 % (Figure 4A), at the PP stage PDX1-expressing cells were 88.88 ± 1.17 % (Figure 4B), and at the EP stage, NGN3-expressing cells were 16.53 ± 7.74 % (Figure 4C). These results showed that the cells in each differentiation stage were a mixed cell population with specific marker(s)-expressing cells and other lineage cells, especially the differentiation efficiency of EP cell stage was low. In order to efficiently generate pancreatic islets, it is necessary to increase the NGN3-expressing EP cells.

Isolation of hiPSC-derived EP cells

本章については、5 年以内に雑誌等で刊行予定のため、非公開。

本章については、5 年以内に雑誌等で刊行予定のため、非公開。

Differentiation into pancreatic islets

本章については、5 年以内に雑誌等で刊行予定のため、非公開。

本章については、5 年以内に雑誌等で刊行予定のため、非公開。

本章については、5 年以内に雑誌等で刊行予定のため、非公開。

Cell growth of *NGN3*-expressing EP cells

I examined whether *NGN3*-expressing cells have the proliferation capacity. While the fraction of proliferation marker Ki67 positive cells in the hiPSCs was high, it dramatically decreased as the progression of differentiation towards the EP cells (Figure 12A, B). At the EP stage, immunostaining with anti-NGN3 and anti-Ki67 antibodies revealed that Ki67 positive cells were hardly found in the NGN3-expressing fraction (0.5 ± 0.1%), whereas 11.6 ± 2.6% of NGN3-negative cells were Ki67 positive (Figure 13A, B).

In addition, the number of sorted *NGN3*-mCherry^{high} cells in suspension culture was significantly reduced after the 2nd passage of culture (Figure 14A, B). These results showed that *NGN3*-mCherry^{high} cells were non-proliferating cells.

Expansion of *NGN3*-mCherry^{high} EP cells

In order to stimulate proliferation of *NGN3*-mCherry^{high} cells, I introduced proliferation promoting genes, SV40LT, hTERT, c-MYC, or BMI1 (Narushima et al., 2005)(Ravassard et al., 2011)(Lee et al., 2003)(Karslioglu et al., 2011)(Dhawan et al., 2009) by using a

lentiviral vector under the control of the EF1α promoter (Figure 15). I found that SV40LT expression induced 2.2 ± 0.3 fold expansion of this cell population in 12 days, whereas expression of hTERT, c-MYC, and BMI1 failed to stimulate the proliferation and the cell numbers declined (Figure 16). These results indicated that SV40LT can effectively induce proliferation of *NGN3*-mCherry^{high} cells.

Reversible expression of SV40LT in *NGN3*-mCherry^{high} EP cells

As NGN3 expression is suppressed in a cell cycle-dependent manner (Solorzano-Vargas et al., 2019), the gene expression of *NGN3*, *NEUROD1*, and *NKX2.2* was decreased in SV40LT expressing *NGN3*-mCherry^{high} cells (data not shown). For this reason, it would be ideal to shut down the expression of SV40LT after the expansion of *NGN3*-mCherry^{high} cells. I constructed a lentivirus vector, SV40LT-loxP, which contained SV40LT flanked by loxP sequences, allowing the removal of SV40LT by Cre recombinase (Figure 17). *NGN3*-mCherry^{high} cells with SV40LT-loxP proliferated about 9.1 ± 1.9 fold after 35 days post-transduction (Figure 18). The gene expression of *NGN3*, *NEUROD1*, and *NKX2.2* was rapidly decreased in SV40LT expressing *NGN3*-mCherry^{high} cells. Expression of an EP cell surface marker, *SUSD2*, was once decreased at the second and third passages but increased again and regained the same level as the

one before proliferation. Importantly, the pancreatic transcription factor *PDX1* (Liu et al., 2014), whose expression was induced at passage 3, was not significantly affected by SV40LT-loxP expression (Figure 19). The results indicated that SV40LT-induced proliferating cells maintained, at least in part, their pancreatic endocrine characteristics.

I then used Cre-expressing lentivirus (LV-Cre) to remove SV40LT in expanded *NGN3*-mCherry^{high} cells. *NGN3*-mCherry^{high} cells with SV40LT-loxP were subsequently transduced with LV-Cre, followed by 10 days in suspension culture (Figure 20). Five days after transduction with LV-Cre transduction, the expression of SV40LT was significantly reduced (Figure 21). And 10 days after transduction with LV-Cre transduction, cell proliferation was terminated (Figure 22). Fluorescence microscopic analysis revealed that LV-Cre-transduced cells exhibited greater NGN3-mCherry fluorescence compared with the control group at day 10 in culture (Figure 23). Furthermore, *NGN3*, *NEUROD1*, and *NKX2.2* gene expression were significantly increased by the removal of the SV40LT gene (Figure 24).

Generation of functional pancreatic islets from expanded *NGN3*-mCherry^{high} cells

Immediately after LV-Cre transduction, *NGN3*-mCherry^{high} cells were cultured in Stage 5 (islet cells) medium for 10 days to induce differentiation to islets. This result showed

that insulin secretion was negative/low and GSIS was not shown (Figure 25A, B). These results suggested that the expression level of NGN3 is important for the differentiation of pancreatic islets. Next, LV-Cre-transduced *NGN3*-mCherry^{high} cells were cultured in Stage 4 (EP cells) medium for 10 days in order to revert the expression of NGN3. And then, these spheroids were differentiated in Stage 5 (islet cells) medium for 10 days (Figure 26A). This result showed that pancreatic islets derived from expanded and LV-Cre-transduced *NGN3*-mCherry^{high} cells exhibited insulin secretion. Importantly, although stimulation index was lower compared to the pancreatic islets without expansion using the original protocol (Figure 11, red bars), they exhibited high insulin secretion and a tendency of insulin secretion in response to glucose (Figure 26B, orange bars). These results suggest that the recovery of NGN3 expression and cell cycle arrest is important for functional pancreatic islet differentiation (Figure 27).

Discussion

Methods of a scalable culture of hPSC-derived β cells

For the clinical use of pancreatic islets derived from hPSCs for diabetes, a stable supply of a large quantity of islets is necessary. However, current protocols to generate islets from human ESCs or iPSCs require multiple differentiation steps, resulting in low and variable efficiency of islets production. As islet transplantation requires a large number of islets, scaling of the production is necessary, the current protocols need to start with a large number of hPSCs to produce islets and hence the whole differentiation processes are extremely costly. Generally, generation of terminally differentiated cells from hPSCs in culture commonly requires multiple steps using expensive cytokines, it is therefore beneficial to derive expandable progenitor cells for a cost effective and simplified method to produce mature cells. In fact, our laboratory previously reported that liver progenitor cells in mouse fetal liver can be propagated and differentiated to both hepatocytes and cholangiocytes *in vitro* (Tanimizu et al., 2003) and that similar expandable bipotential cells can be derived from hiPSCs *in vitro* (Kido et al., 2015). However, unlike liver progenitors during development, there has been no report showing such expandable islet progenitors during embryonic development, while both liver and pancreas are derived

from the foregut endoderm. Consistently, along with the stepwise differentiation of hiPSCs to pancreatic islet cells the proliferation potential was dramatically reduced. Although I tried to expand EP cells in different culture conditions, I was unable to find a condition to enhance proliferation of such cells *in vitro*. I therefore attempted to stimulate proliferation of EP cells by introducing several proliferation enhancing genes using lentivirus vector.

Relationship of NGN3 and cell proliferation

Because differentiation efficiency was notably reduced after the PP cell stage (Stage 4-5) in the stepwise β cell differentiation protocol (Sharon et al., 2019)(Nair et al., 2019) and $NGN3^+$ EP cells differentiated to mature β cells with GSIS, I investigated the possibility to expand $NGN3^+$ EP cells. Among SV40LT, hTERT, c-MYC, and BMI1 genes that are known to promote cell growth, only SV40LT was able to stimulate proliferation of $NGN3^+$ EP cells. The positive role of SV40LT for the proliferation of $NGN3^+$ EP cells may be explained as follows; NGN3 recruits Cyclin-dependent kinase inhibitor 1 (Cdkn1a) that induces cell cycle arrest at the G1 phase by inhibiting cyclin dependent kinases (CDKs) (Miyatsuka et al., 2011) and SV40LT releases G1 arrest by binding to Retinoblastoma (RB) protein, a downstream target of CDKs (Ludlow et al., 1990),

whereas hTERT, c-MYC, and BMI1 are considered to act upstream of CDKs (Bringold & Serrano, 2000).

This study showed that *NGN3*-mCherry^{high} cells could be cultured for 35 days after the transduction of SV40LT, and that these cells continuously proliferated. However, since generally cells do not have potential to proliferate indefinitely *in vitro*, SV40LT-transduced *NGN3*-mCherry^{high} cells would not proliferate for long-term. hTERT is well known for cell immortalization and long-term growth (Lundberg et al., 2000). Thus, I considered the possibility that co-transduction of hTERT into *NGN3*-mCherry^{high} cells could promote long-term proliferation. In fact, a previous report showed that human cementifying fibroma cell lines were established by transduction of SV40LT and hTERT, which proliferated stably for long term (Kudo et al., 2002). In my preliminary experiment, co-transduction of SV40LT and hTERT into *NGN3*-mCherry^{high} cells promoted cell proliferation more than SV40LT alone at day 16 of culture. Therefore, transduction of SV40LT and hTERT may be effective for long-term cell growth of *NGN3*-mCherry^{high} cells.

Proliferation vs differentiation of EP cells

Although SV40LT enhances proliferation of $NGN3^{+}$ EP cells, proliferation and differentiation were trade-offs and the forced proliferation of EP cells resulted in the loss of differentiation potential. NGN3 is a cell fate commitment factor for the endocrine-lineage in the pancreas (Gradwohl et al., 2000). In the development of the murine pancreas, Ngn3-low expressing epithelial cells arise from the trunk region consisting of the common progenitors of endocrine and ductal cells (Shih et al., 2012). The epithelial cells increase gradually the expression level of Ngn3 along with the detachment from the ductal structure and differentiate into mature endocrine cells (Bankaitis et al., 2018). The increased expression of Ngn3 induces cell cycle arrest (Bechard & Wright, 2017). Consistently, I showed in this study that SV40LT induced cell proliferation and reduced the expression of *NGN3*, *NEUROD1*, and *NKX2.2*, key factors for β cell maturation. However, SV40LT expression did not significantly affect the expression of *SUSD2* and *PDX1* that are important for pancreatic endocrine cells, suggesting that SV40LT maintains partially the characteristics of the pancreatic lineage. Importantly, the removal of SV40LT rapidly rescued the NGN3 expression and potential to differentiate to mature islets. As mouse Ngn3-low cells adjacent to the ductal region expresses Sox9 in fetal pancreas. And *SOX9* was increased in parallel with reduction of NGN3 expression in

SV40LT-transduced *NGN3*-mCherry^{high} cells (data not shown), it is tempting to speculate that SV40LT-transduced *NGN3*-mCherry^{high} cells with reduced NGN3 expression are reversibly dedifferentiated into the cells similar to Ngn3-low trunk cells in the mouse fetal pancreas.

Conclusion

For the clinical application of type 1 diabetes, stable supply of pancreatic islets or β cells is necessary. This study demonstrated that EP cells defined by the expression of *NGN3* were able to differentiate into functional pancreatic islets and that the transduction of SV40LT was effective for the expansion of EP cells. Although SV40LT suppressed the gene expression of *NGN3* and differentiation toward islets, shutdown of SV40LT expression rescued *NGN3* expression, allowing the expanded EP cells to differentiate to functional pancreatic islets exhibiting a tendency of insulin secretion in response to glucose.

In conclusion, the results in this study will lead to a cost effective means to expand EP cells to produce a large number of functional islets from PSCs for clinical use.

References

Arda, H.E., Li, L., Tsai, J., et al. (2016). Age-dependent pancreatic gene regulation reveals mechanisms governing human β cell function. *Cell Metab.* **23**, 909–920.

Ashcroft, F.M., & Rorsman, P. (2012). Diabetes mellitus and the β cell: The last ten years. *Cell* **148**, 1160–1171.

Bankaitis, E.D., Bechard, M.E., Gu, G., Magnuson, M.A., & Wright, C.V.E. (2018). ROCK-nmMyoII, Notch and Neurog3 gene-dosage link epithelial morphogenesis with cell fate in the pancreatic endocrine-progenitor niche. *Development* **145**, dev162115.

Bechard, M.E., & Wright, C.V.E. (2017). New ideas connecting the cell cycle and pancreatic endocrine-lineage specification. *Cell Cycle* **16**, 301–303.

Benitez, C.M., Goodyer, W.R., & Kim, S.K. (2012). Deconstructing pancreas developmental biology. *Cold Spring Harb. Perspect. Biol.* **4**, 1–17.

Bringold, F., & Serrano, M. (2000). Tumor suppressors and oncogenes in cellular senescence. *Exp. Gerontol.* **35**, 317–329.

Collombat, P., Mansouri, A., Hecksher-Sørensen, J., Serup, P., Krull, J., Gradwohl, G., & Gruss, P. (2003). Opposing actions of Arx and Pax4 in endocrine pancreas development. *Genes Dev.* **17**, 2591–2603.

D'Amour, K.A., Bang, A.G., Eliazer, S., Kelly, O.G., Agulnick, A.D., Smart, N.G., Moorman, M.A., Kroon, E., Carpenter, M.K., & Baetge, E.E. (2006). Production of pancreatic hormone-expressing endocrine cells from human embryonic stem cells. *Nat. Biotechnol.* **24**, 1392–1401.

Dhawan, S., Tschen, S.I., & Bhushan, A. (2009). Bmi-1 regulates the Ink4a/Arf locus to control pancreatic β-cell proliferation. *Genes Dev.* **23**, 906–911.

Gallagher, G.R., Brehm, M.A., Finberg, R.W., Barton, B.A., Shultz, L.D., Greiner, D.L., Bortell, R., & Wang, J.P. (2015). Viral infection of engrafted human islets leads to diabetes. *Diabetes* **64**, 1358–1369.

Gao, T., McKenna, B., Li, C., et al. (2014). Pdx1 maintains β cell identity and function by repressing an α cell program. *Cell Metab.* **19**, 259–271.

Gradwohl, G., Dierich, A., LeMeur, M., & Guillemot, F. (2000). neurogenin3 is required for the development of the four endocrine cell lineages of the pancreas. *Proc. Natl. Acad. Sci. U. S. A.* **97**, 1607–1611.

Gu, G., Dubauskaite, J., & Melton, D.A. (2002). Direct evidence for the pancreatic lineage: NGN3^{+} cells are islet progenitors and are distinct from duct progenitors. *Development* **129**, 2447–2457.

Jain, R., & Lammert, E. (2009). Cell-cell interactions in the endocrine pancreas. *Diabetes, Obes. Metab.* **11**, 159–167.

Jiang, W., Hua, R., Wei, M., Li, C., Qiu, Z., Yang, X., & Zhang, C. (2015). An optimized method for high-titer lentivirus preparations without ultracentrifugation. *Sci. Rep.* **5**, 13875.

Karslioglu, E., Kleinberger, J.W., Salim, F.G., Cox, A.E., Takane, K.K., Scott, D.K., & Stewart, A.F. (2011). cMyc is a principal upstream driver of β-cell proliferation in rat insulinoma cell lines and is an effective mediator of human β-cell replication. *Mol. Endocrinol.* **25**, 1760–1772.

Kawaguchi, Y., Cooper, B., Gannon, M., Ray, M., MacDonald, R.J., & Wright, C.V.E. (2002). The role of the transcriptional regulator Ptf1a in converting intestinal to pancreatic progenitors. *Nat. Genet.* **32**, 128–134.

Kido, T., Koui, Y., Suzuki, K., Kobayashi, A., Miura, Y., Chern, E.Y., Tanaka, M., & Miyajima, A. (2015). CPM is a useful cell surface marker to isolate expandable bi-

potential liver progenitor cells derived from human iPS cells. *Stem Cell Reports* **5**, 508–515.

Kimura, A., Toyoda, T., Nishi, Y., Nasu, M., Ohta, A., & Osafune, K. (2017). Small molecule AT7867 proliferates PDX1-expressing pancreatic progenitor cells derived from human pluripotent stem cells. *Stem Cell Res.* **24**, 61–68.

Kojima, N., Takeuchi, S., & Sakai, Y. (2014). Engineering of pseudoislets: Effect on insulin secretion activity by cell number, cell population, and microchannel networks. *Transplant. Proc.* **46**, 1161–1165.

Kondo, Y., Toyoda, T., Inagaki, N., & Osafune, K. (2018). iPSC technology-based regenerative therapy for diabetes. *J. Diabetes Investig.* **9**, 234–243.

Konstantinova, I., & Lammert, E. (2004). Microvascular development: Learning from pancreatic islets. *BioEssays* **26**, 1069–1075.

Krah, N.M., De La O, J.-P., Swift, G.H., Hoang, C.Q., Willet, S.G., Chen Pan, F., Cash, G.M., Bronner, M.P., Wright, C.V., MacDonald, R.J., & Murtaugh, L.C. (2015). The acinar differentiation determinant PTF1A inhibits initiation of pancreatic ductal adenocarcinoma. *Elife* **4**, 1–25.

Kroon, E., Martinson, L.A., Kadoya, K., Bang, A.G., Kelly, O.G., Eliazer, S., Young, H., Richardson, M., Smart, N.G., Cunningham, J., Agulnick, A.D., D'Amour, K.A.,

Carpenter, M.K., & Baetge, E.E. (2008). Pancreatic endoderm derived from human embryonic stem cells generates glucose-responsive insulin-secreting cells in vivo. *Nat. Biotechnol.* **26**, 443–452.

Kudo, Y., Hiraoka, M., Kitagawa, S., Miyauchi, M., Kakuo, S., Zhao, M., Ide, T., & Takata, T. (2002). Establishment of human cementifying fibroma cell lines by transfection with temperature-sensitive simian virus-40 T-antigen gene and hTERT gene. *Bone* **30**, 712–717.

Lee, K.M., Nguyen, C., Ulrich, A.B., Pour, P.M., & Ouellette, M.M. (2003). Immortalization with telomerase of the Nestin-positive cells of the human pancreas. *Biochem. Biophys. Res. Commun.* **301**, 1038–1044.

Liu, H., Yang, H., Zhu, D., et al. (2014). Systematically labeling developmental stage-specific genes for the study of pancreatic β -cell differentiation from human embryonic stem cells. *Cell Res.* **24**, 1181–1200.

Ludlow, J.W., Shon, J., Pipas, J.M., Livingston, D.M., & DeCaprio, J.A. (1990). The retinoblastoma susceptibility gene product undergoes cell cycle-dependent dephosphorylation and binding to and release from SV40 large T. *Cell* **60**, 387–396.

Lundberg, A.S., Hahn, W.C., Gupta, P., & Weinberg, R.A. (2000). Genes involved in senescence and immortalization. *Curr. Opin. Cell Biol.* **12**, 705–709.

Mathis, D., Vence, L., & Benoist, C. (2001). β-Cell death during progression to diabetes. *Nature* **414**, 792–798.

Miyatsuka, T., Kosaka, Y., Kim, H., & German, M.S. (2011). Neurogenin3 inhibits proliferation in endocrine progenitors by inducing Cdkn1a. *Proc. Natl. Acad. Sci. U. S. A.* **108**, 185–190.

Nair, G.G., Liu, J.S., Russ, H.A., et al. (2019). Recapitulating endocrine cell clustering in culture promotes maturation of human stem-cell-derived β cells. *Nat. Cell Biol.* **21**, 263–274.

Nakano, Y., Negishi, N., Gocho, S., Mine, T., Sakurai, Y., Yazawa, M., Abe, K., Yagita, H., Habu, S., Kageyama, R., Kawaguchi, Y., & Hozumi, K. (2015). Disappearance of centroacinar cells in the Notch ligand-deficient pancreas. *Genes to Cells* **20**, 500–511.

Narushima, M., Kobayashi, N., Okitsu, T., et al. (2005). A human beta-cell line for transplantation therapy to control type 1 diabetes. *Nat. Biotechnol.* **23**, 1274–1282.

Naya, F.J., Huang, H.P., Qiu, Y., Mutoh, H., DeMayo, F.J., Leiter, A.B., & Tsai, M.J. (1997). Diabetes, defective pancreatic morphogenesis, and abnormal enteroendocrine differentiation in BETA2/NeuroD-deficient mice. *Genes Dev.* **11**, 2323–2334.

Offield, M.F., Jetton, T.L., Labosky, P.A., Ray, M., Stein, R.W., Magnuson, M.A., Hogan, B.L.M., & Wright, C.V.E. (1996). PDX-1 is required for pancreatic outgrowth and differentiation of the rostral duodenum. *Development* **122**, 983–995.

Pagliuca, F.W., Millman, J.R., Gürtler, M., Segel, M., Van Dervort, A., Ryu, J.H., Peterson, Q.P., Greiner, D., & Melton, D.A. (2014). Generation of functional human pancreatic β cells in vitro. *Cell* **159**, 428–439.

Ravassard, P., Hazhouz, Y., Pechberty, S., Bricout-Neveu, E., Armanet, M., Czernichow, P., & Scharfmann, R. (2011). A genetically engineered human pancreatic β cell line exhibiting glucose-inducible insulin secretion. *J. Clin. Invest.* **121**, 3589–3597.

Rezania, A., Bruin, J.E., Arora, P., Rubin, A., Batushansky, I., Asadi, A., O'Dwyer, S., Quiskamp, N., Mojibian, M., Albrecht, T., Yang, Y.H.C., Johnson, J.D., & Kieffer, T.J. (2014). Reversal of diabetes with insulin-producing cells derived in vitro from human pluripotent stem cells. *Nat. Biotechnol.* **32**, 1121–1133.

Russ, H.A., Parent, A. V, Ringler, J.J., Hennings, T.G., Nair, G.G., Shveygert, M., Guo, T., Puri, S., Haataja, L., Cirulli, V., Blelloch, R., Szot, G.L., Arvan, P., & Hebrok, M. (2015). Controlled induction of human pancreatic progenitors produces functional beta-like cells in vitro. *EMBO J.* **34**, 1759–1772.

Sakaue-Sawano, A., Kurokawa, H., Morimura, T., Hanyu, A., Hama, H., Osawa, H., Kashiwagi, S., Fukami, K., Miyata, T., Miyoshi, H., Imamura, T., & Ogawa, M. (2008). Visualizing Spatiotemporal Dynamics of Multicellular Cell-Cycle Progression. *Cell* **132**, 487–498.

Sander, M., Sussel, L., Conners, J., Scheel, D., Kalamaras, J., Dela Cruz, F., Schwitzgebel, V., Hayes-Jordan, A., & German, M. (2000). Homeobox gene Nkx6.1 lies downstream of Nkx2.2 in the major pathway of β-cell formation in the pancreas. *Development* **127**, 5533–5540.

Schaffer, A.E., Freude, K.K., Nelson, S.B., & Sander, M. (2010). Nkx6 Transcription Factors and Ptf1a Function as Antagonistic Lineage Determinants in Multipotent Pancreatic Progenitors. *Dev. Cell* **18**, 1022–1029.

Senior, P.A., & Pettus, J.H. (2019). Stem cell therapies for Type 1 diabetes: current status and proposed road map to guide successful clinical trials. *Diabet. Med.* **36**, 297–307.

Shapiro, A.M.J., Lakey, J.R.T., Ryan, E.A., Korbutt, G.S., Toth, E., Warnock, G.L., Kneteman, N.M., & Rajotte, R. V. (2000). Islet transplantation in seven patients with type 1 diabetes mellitus using a glucocorticoid-free immunosuppressive regimen. *N. Engl. J. Med.* **343**, 230–238.

Shapiro, A.M.J., Ricordi, C., Hering, B.J., et al. (2006). International trial of the Edmonton protocol for islet transplantation. *N. Engl. J. Med.* **355**, 1318–1330.

Sharon, N., Vanderhooft, J., Straubhaar, J., Mueller, J., Chawla, R., Zhou, Q., Engquist, E.N., Trapnell, C., Gifford, D.K., & Melton, D.A. (2019). Wnt Signaling Separates the Progenitor and Endocrine Compartments during Pancreas Development. *Cell Rep.* **27**, 2281–2291.

Shih, H.P., Kopp, J.L., Sandhu, M., Dubois, C.L., Seymour, P.A., Grapin-Botton, A., & Sander, M. (2012). A Notch-dependent molecular circuitry initiates pancreatic endocrine and ductal cell differentiation. *Development* **139**, 2488–2499.

Sneddon, J.B., Borowiak, M., & Melton, D.A. (2012). Self-renewal of embryonic-stem-cell-derived progenitors by organ-matched mesenchyme. *Nature* **491**, 765–768.

Solorzano-Vargas, R.S., Bjerknes, M., Wu, S.V., Wang, J., Stelzner, M., Dunn, J.C.Y., Dhawan, S., Cheng, H., Georgia, S., & Martín, M.G. (2019). The cellular regulators PTEN and BMI1 help mediate NEUROGENIN-3–induced cell cycle arrest. *J. Biol. Chem.* **294**, 15182–15192.

Soria, B., Roche, E., Berná, G., León-Quinto, T., Reig, J.A., & Martín, F. (2000). Insulin-Secreting Cells Derived From in Streptozotocin-Induced Diabetic Mice Embryonic Stem Cells Normalize Glycemia. *Diabetes* **49**, 157–162.

Sussel, L., Kalamaras, J., Hartigan-O'Connor, D.J., Meneses, J.J., Pedersen, R.A., Rubenstein, J.L.R., & German, M.S. (1998). Mice lacking the homeodomain transcription factor Nkx2.2 have diabetes due to arrested differentiation of pancreatic β cells. *Development* **125**, 2213–2221.

Tanimizu, N., Nishikawa, M., Saito, H., Tsujimura, T., & Miyajima, A. (2003). Isolation of hepatoblasts based on the expression of Dlk/Pref-1. *J. Cell Sci.* **116**, 1775–1786.

Taylor, B.L., Liu, F.F., & Sander, M. (2013). Nkx6.1 Is Essential for Maintaining the Functional State of Pancreatic Beta Cells. *Cell Rep.* **4**, 1262–1275.

Traub, S., Meier, D.T., Schulze, F., Dror, E., Nordmann, T.M., Goetz, N., Koch, N., Dalmas, E., Stawiski, M., Makshana, V., Thorel, F., Herrera, P.L., Böni-Schnetzler, M., & Donath, M.Y. (2017). Pancreatic α Cell-Derived Glucagon-Related Peptides Are Required for β Cell Adaptation and Glucose Homeostasis. *Cell Rep.* **18**, 3192–3203.

Veres, A., Faust, A.L., Bushnell, H.L., Engquist, E.N., Kenty, J.H.R., Harb, G., Poh, Y.C., Sintov, E., Gürtler, M., Pagliuca, F.W., Peterson, Q.P., & Melton, D.A. (2019). Charting cellular identity during human in vitro β-cell differentiation. *Nature* **569**, 368–373.

Yabe, S.G., Fukuda, S., Takeda, F., Nashiro, K., Shimoda, M., & Okochi, H. (2017). Efficient Generation of Functional Pancreatic β Cells from Human iPS Cells. *J. Diabetes* **9**, 168–179.

Yabe, S.G., Fukuda, S., Nishida, J., Takeda, F., Nashiro, K., & Okochi, H. (2019). Induction of functional islet-like cells from human iPS cells by suspension culture. *Regen. Ther.* **10**, 69–76.

Yamashita-Sugahara, Y., Matsumoto, M., Ohtaka, M., Nishimura, K., Nakanishi, M., Mitani, K., & Okazaki, Y. (2016). An inhibitor of fibroblast growth factor receptor-1 (FGFR1) promotes late-stage terminal differentiation from $NGN3^+$ pancreatic endocrine progenitors. *Sci. Rep.* **6**, 35908.

Zhou, Q., & Melton, D.A. (2018). Pancreas regeneration. *Nature* **557**, 351–358.

Zhu, Z., Li, Q. V., Lee, K., Rosen, B.P., González, F., Soh, C.L., & Huangfu, D. (2016). Genome Editing of Lineage Determinants in Human Pluripotent Stem Cells Reveals Mechanisms of Pancreatic Development and Diabetes. *Cell Stem Cell* **18**, 755–768.

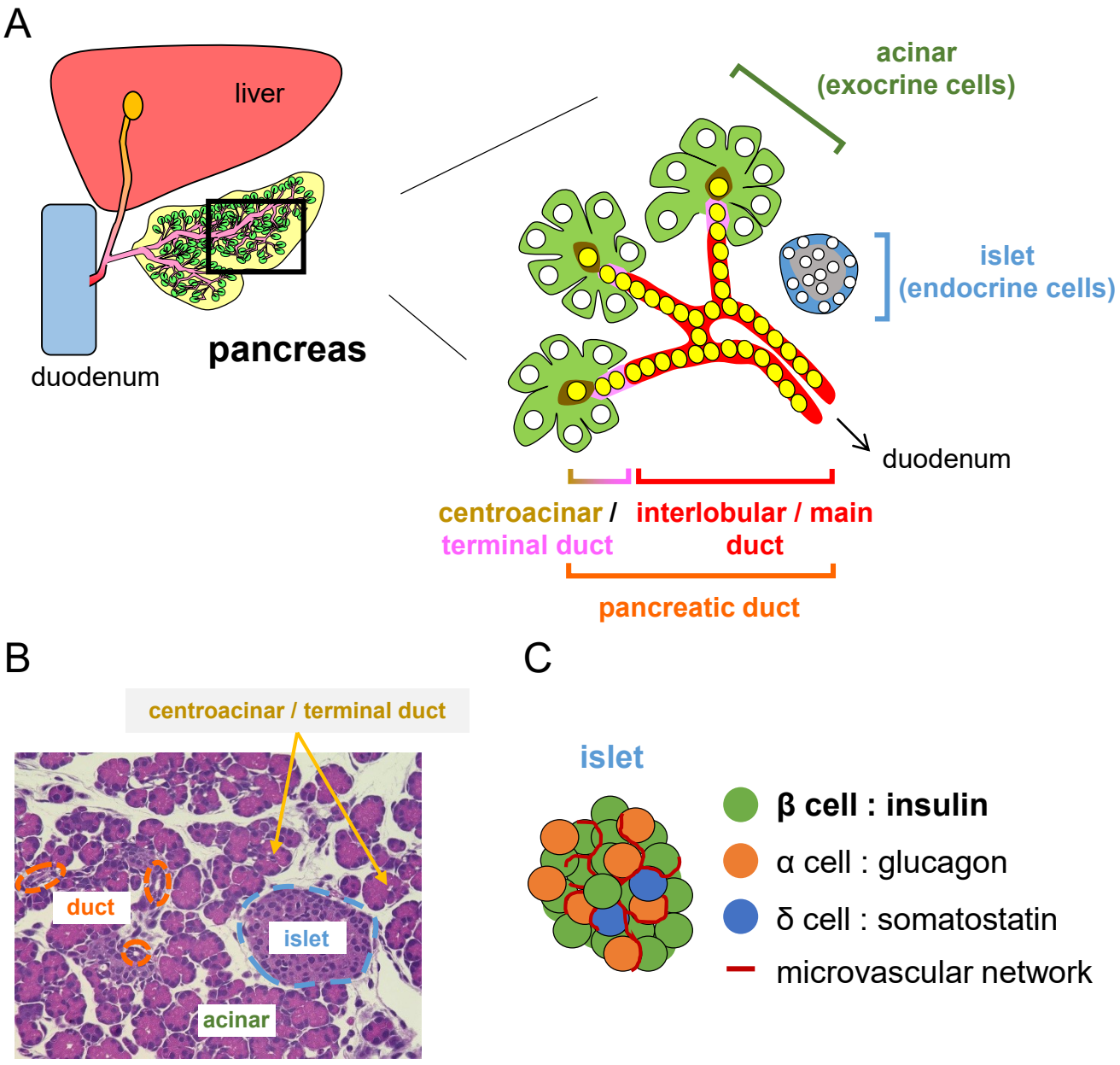

Figure 1. Structure of the pancreas and pancreatic islet

(A) Structure of the pancreas. Pancreatic juice, including digestive enzymes, is secreted from the exocrine cells and is released into the duodenum through pancreatic ducts. The acinar structure is consisted of exocrine cells and connects to centroacinar / terminal duct, and the islet structure is composed of endocrine cells. (B) Hematoxylin and eosin (H&E) staining of pancreas sections from adult mouse. (C) Structure of the islet. The pancreatic islet is composed of several hormone-producing cells such as β cells, α cells, and δ cells and microvascular network.

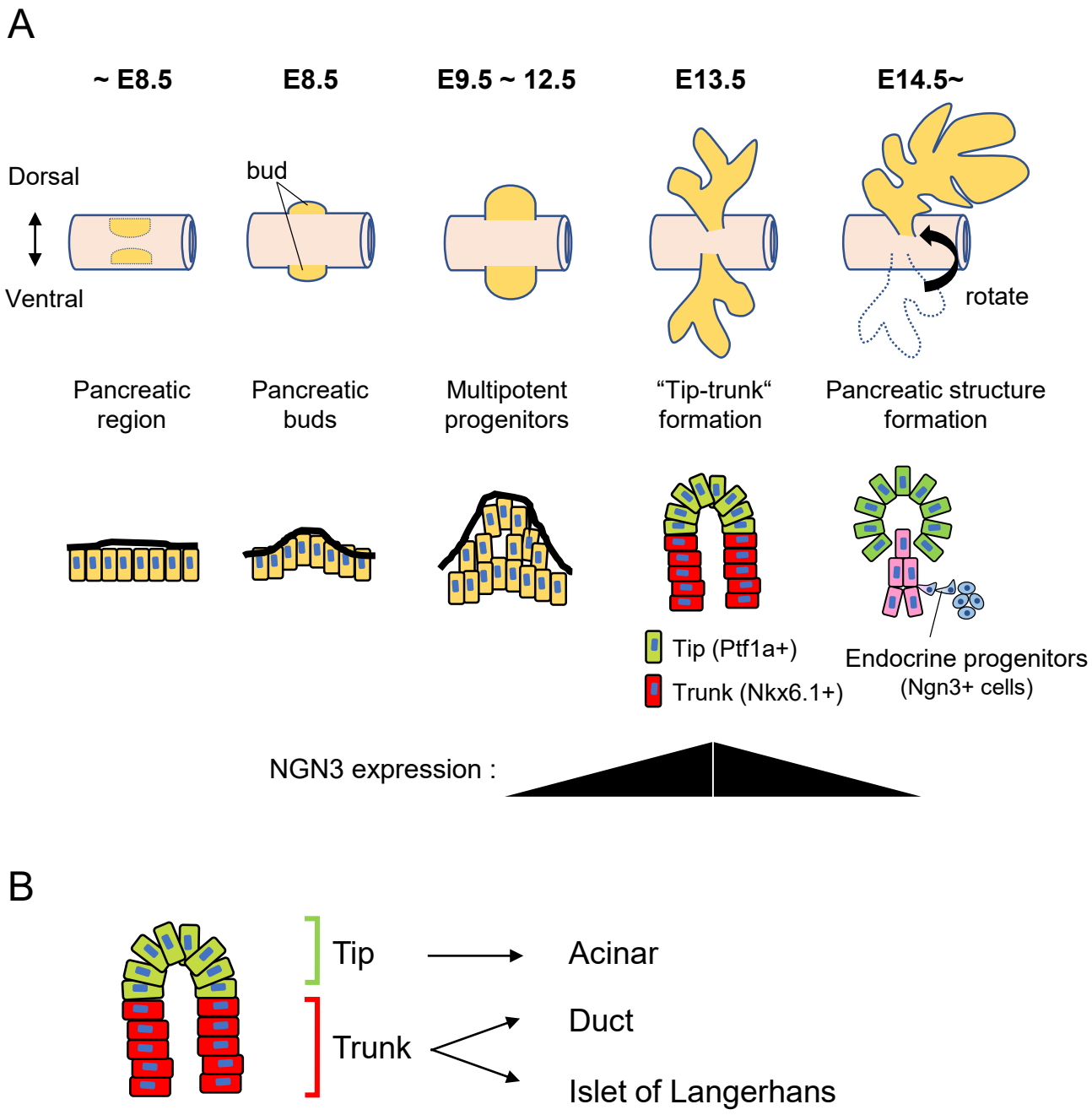

Figure 2. Pancreatic development in the mouse

(A) Pancreatic development in embryonic day (*E*) 8.5 to E14.5. Dorsal and ventral pancreatic buds arise E8.5. From E9.5 to E12.5, $Pdx1^{+}$/$Ptf1a^{+}$/$Nkx6.1^{+}$ multipotent pancreatic progenitor cells expand. Each pancreatic bud forms a branching structure and is compartmentalized into the tip-trunk region in E13.5. At around E14.5, the ventral pancreatic bud rotates to dorsally, and these buds fuse to form one pancreas. (B) "tip-trunk" region development. The tip region differentiates the exocrine acinar. The trunk region mostly becomes the duct structure, and some cells differentiate endocrine cells cluster islet of Langerhans.

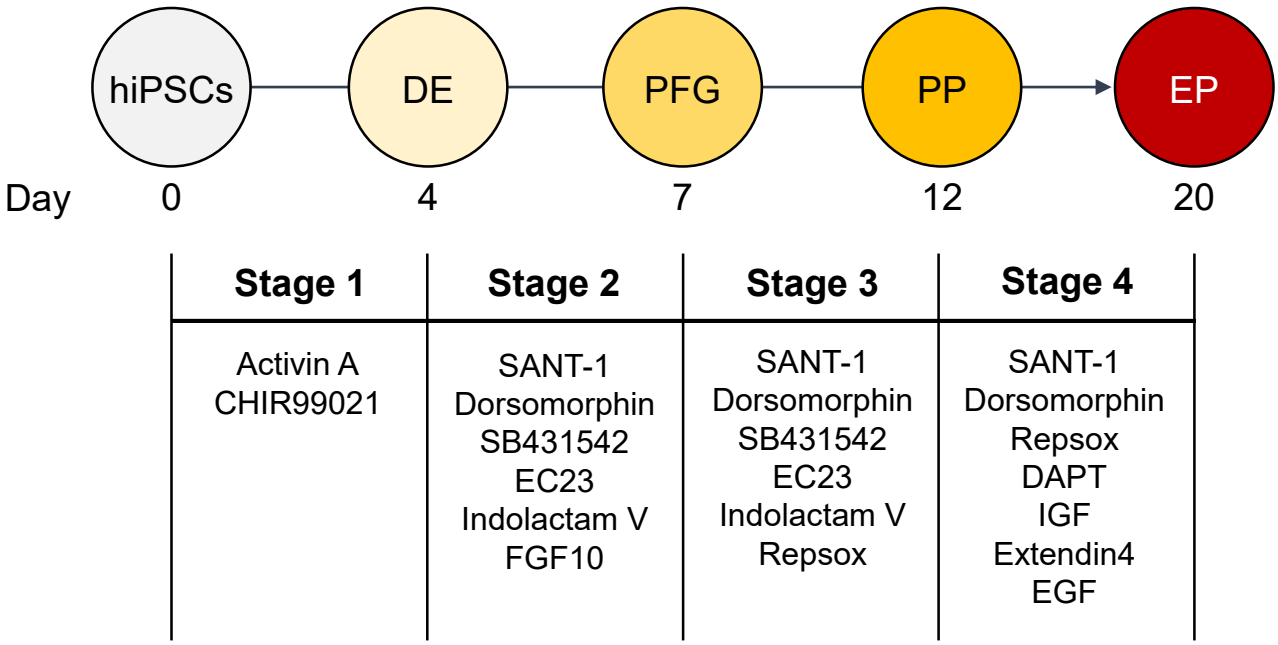

Figure 3. Summary of the four stepwise differentiation protocol from human iPS cells

hiPSCs, human induced pluripotent stem cells; DE, definitive endoderm; PFG, posterior foregut; PP, pancreatic progenitor; EP, endocrine progenitor; FGF10, fibroblast growth factor 10; IGF, insulin-like growth factor ; EGF, epidermal growth factor.

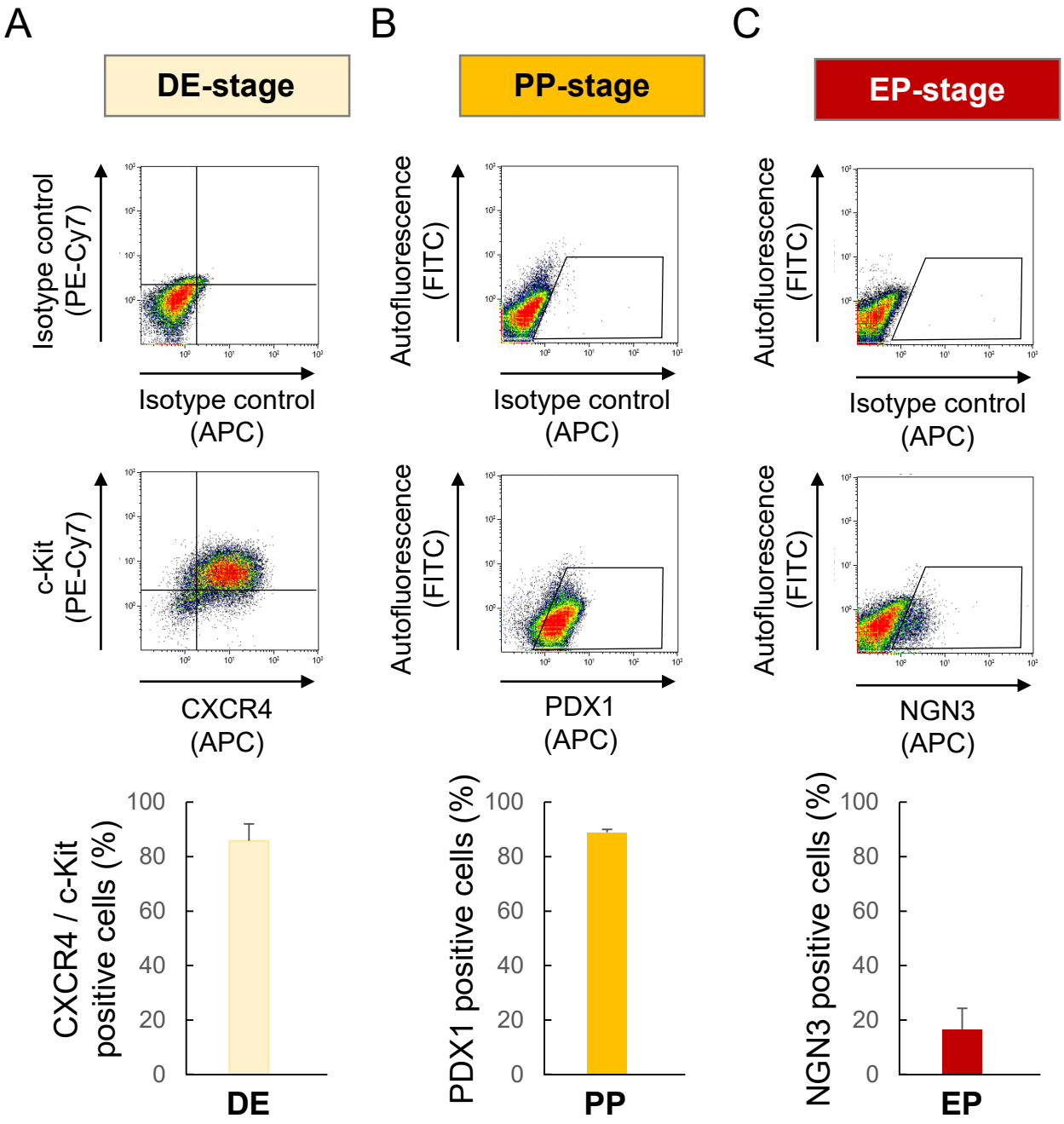

Figure 4. Differentiation efficiency of each stage by flow cytometry analysis

(A-C) Flow cytometry analysis of the stage specific markers were performed. Ratio of CXCR4 and c-Kit double positive cells in definitive endoderm (*DE*)-stage (A), PDX1 positive cells in pancreatic progenitor (*PP*)-stage (B), NGN3 positive cells in endocrine progenitor (*EP*)-stage (C). Each gate defined by isotype negative control. Error bar represents the mean + SD of four independent experiments.

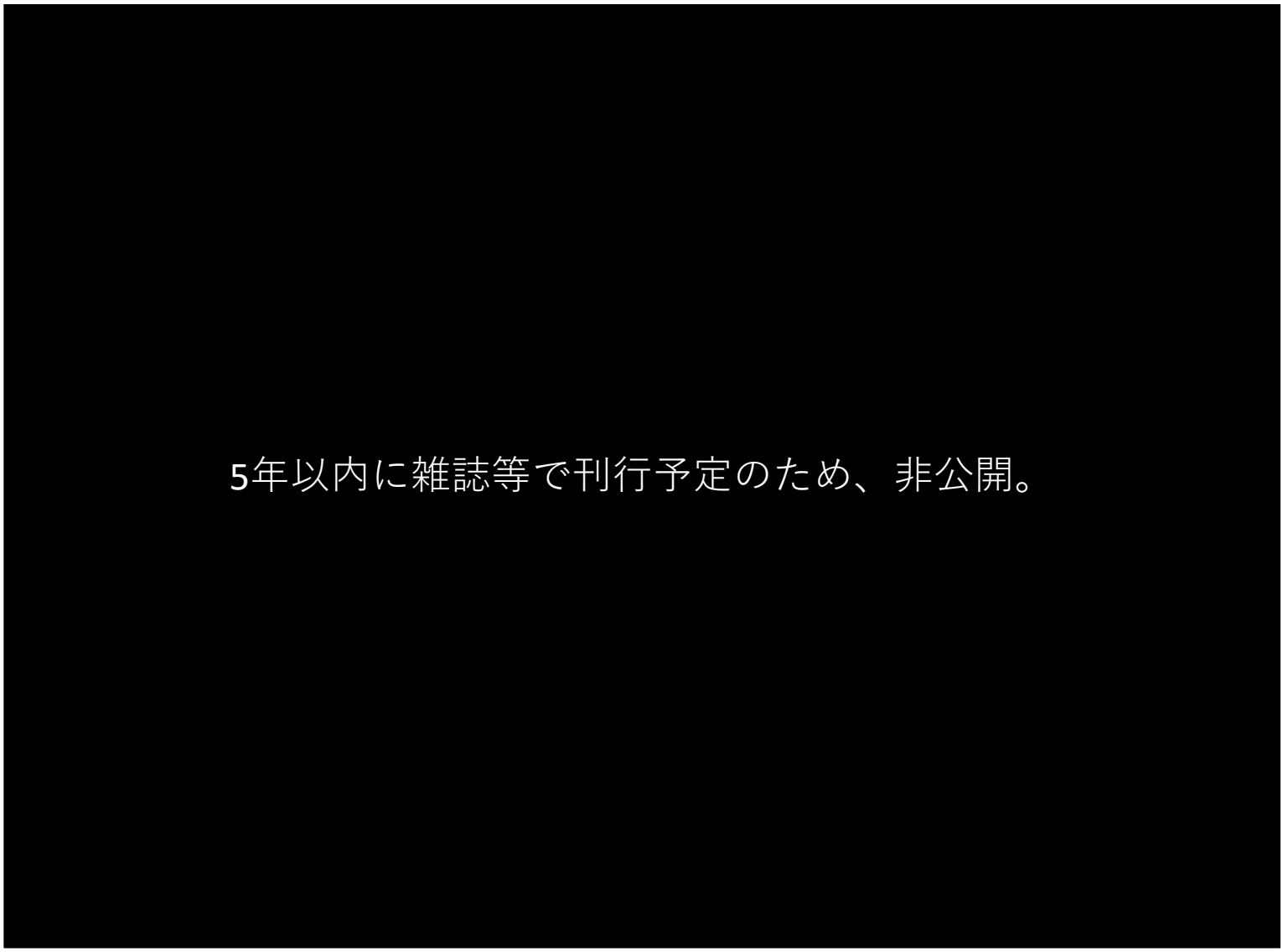

Figure 5. Double knock-in *INS*-Venus/*NGN3*-mCherry (hIveNry) hiPSC-line

(A) Schematic illustration of differentiate into pancreatic islets from hiPSCs using hIveNry cell-line. In hIveNry cells, Venus and mCherry cDNA were inserted under the control of *INS* and *NGN3* promoter at the ATG of the coding region, respectively (Yamashita-Sugahara et al., 2016). (B) The live cell picture of EP-stage cells differentiated from hIveNry hiPSCs by fluorescence microscopy. Scale bars, 100 μm. *hiPSCs*, human induced pluripotent stem cells; *DE*, definitive endoderm; *PFG*, posterior foregut; *PP*, pancreatic progenitor; *EP*, endocrine progenitor; *NGN3*, Neurogenin3; *INS*, Insulin.

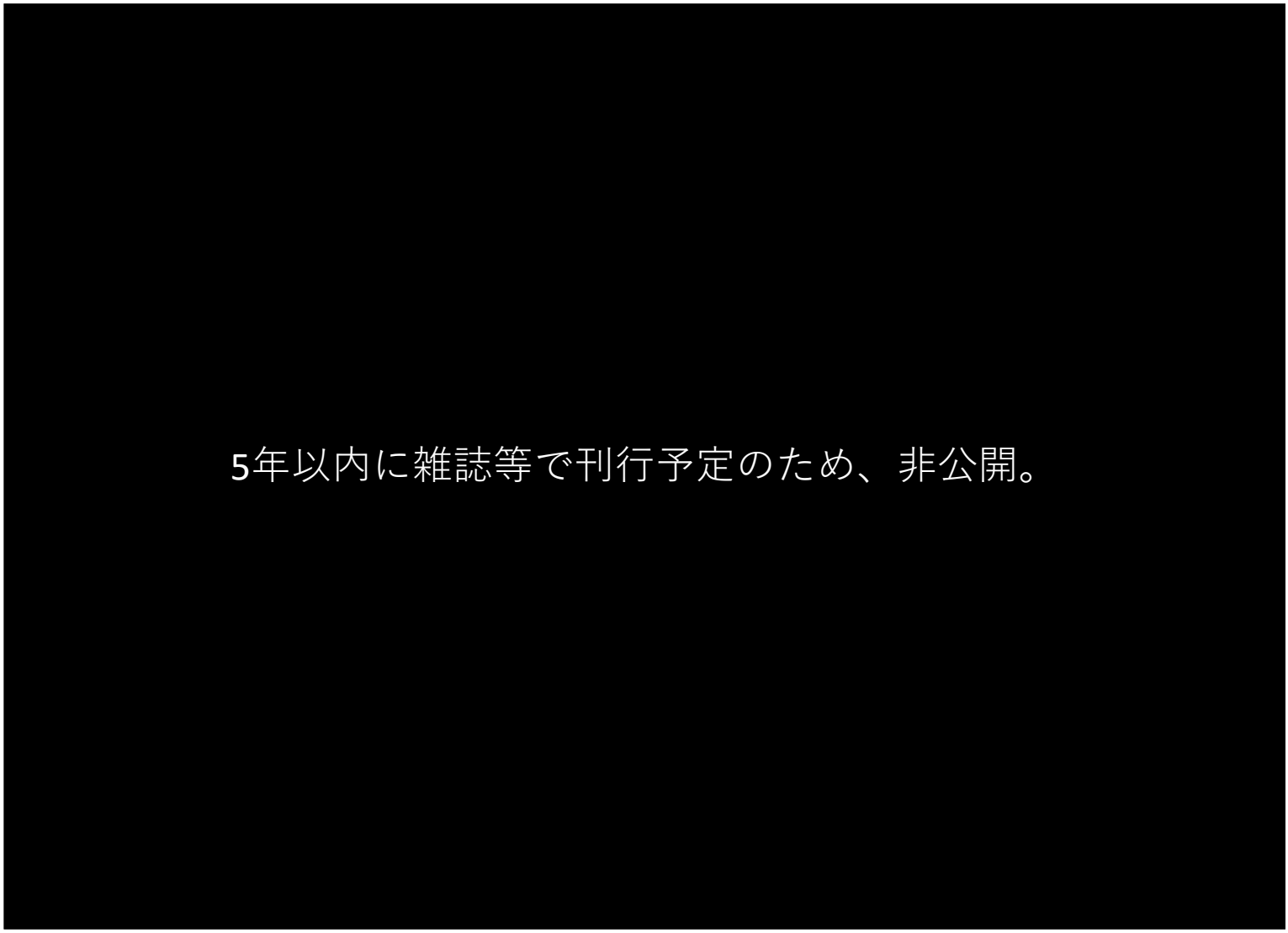

Figure 6. Purification of hiPSC-derived EP cells by using *NGN3*-mCherry reporter

(A) Flow cytometry analysis of *NGN3*-mCherry expression was performed in EP-stage cells derived from hiPSCs. EP-stage cells were divided into the following three fraction by expression of mCherry, *NGN3*-mCherry(-), *NGN3*-mCherry^{low}, and *NGN3*-mCherry^{high}. (B) The live cell picture on day 1 in suspension culture after cell sort by fluorescence microscopy. Left panels, mCherry fluorescence; right panels, brightfield. Scale bars, 100 μm.

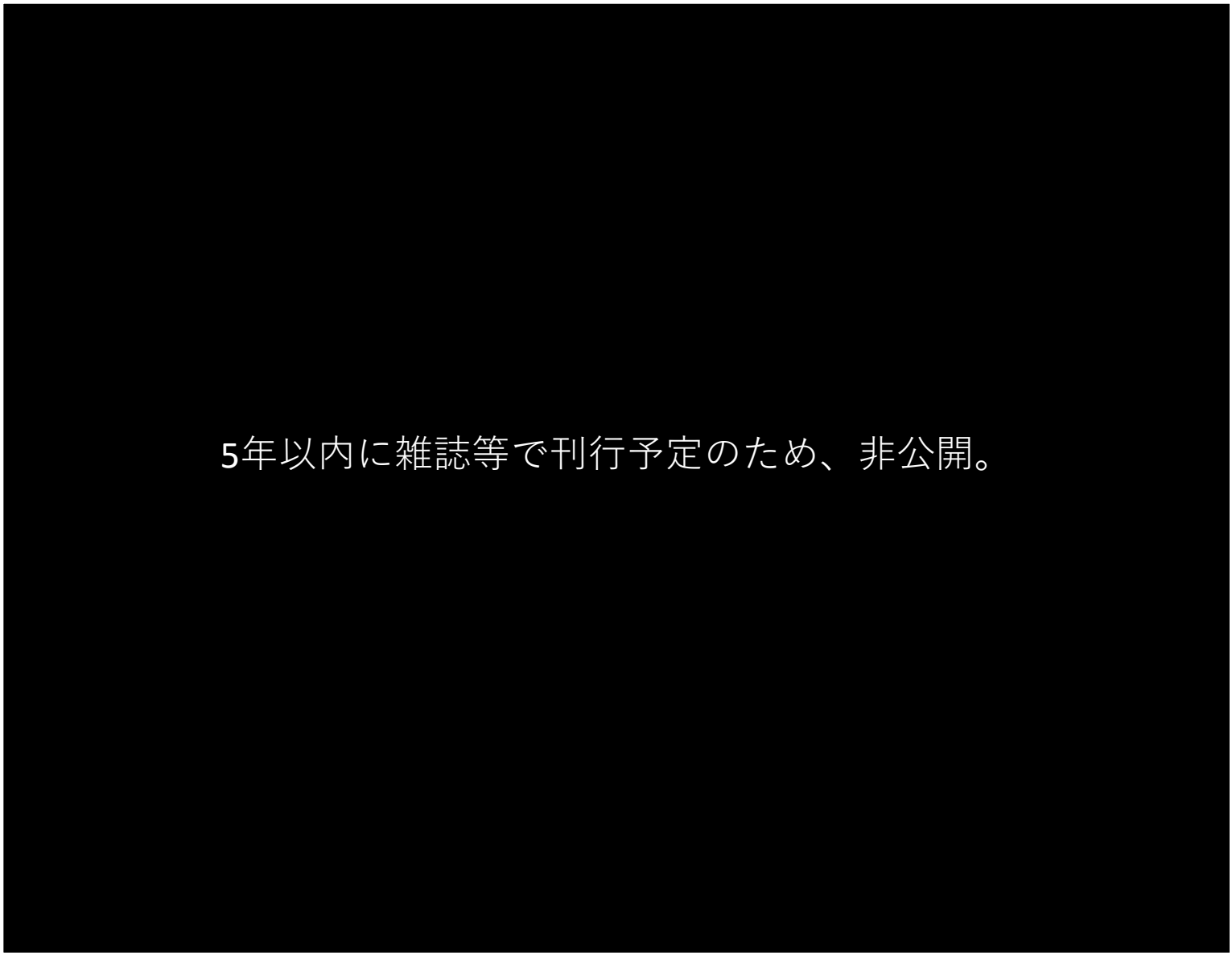

Figure 7. Gene expression analysis of EP and PP markers

(A & B) mRNA expression was analyzed by qRT-PCR and shown are the relative expression levels of the EP marker gene *NGN3*, *NEUROD1*, and *NKX2.2* (A) and the PP gene *PDX1* (B), in pre-sorted, *NGN3*-mCherry(-), *NGN3*-mCherry^{low}, and *NGN3*-mCherry^{high} cells. Expression level of each gene is shown as relative expression level of averaged pre-sorted sample as 1.0. Error bar represents the mean + SD of 4 independent experiments. Statistical analysis was performed using the Turkey-Kramer test. * and **, significantly different from each of the other three fractions. *P < 0.05, ** P < 0.01.

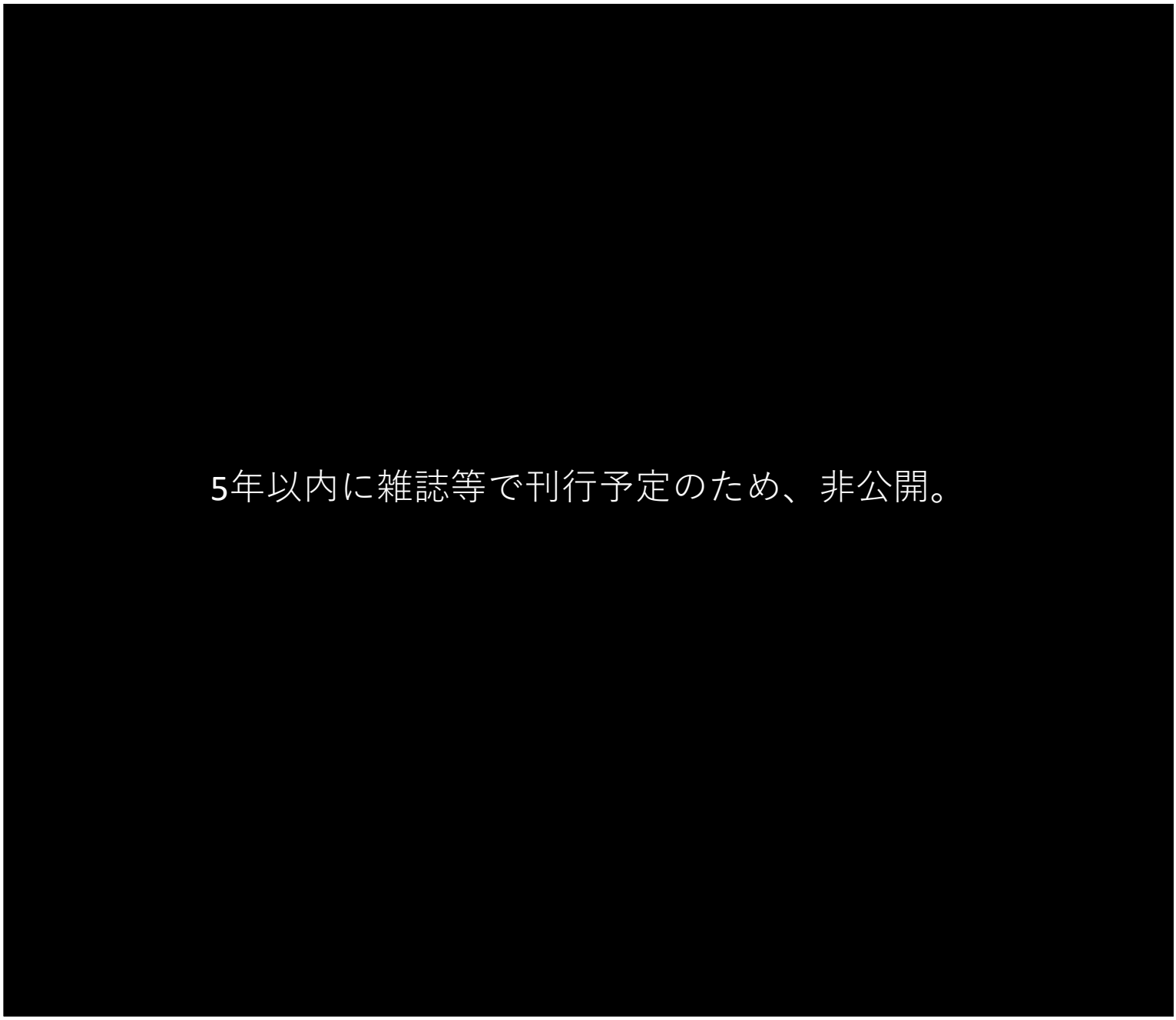

Figure 8. Differentiation of EP cells into pancreatic islet-like structures

(A) Summary of the differentiation protocol from EP cells to islets. (B) Representative images of hiPSC-derived islets from pre-sorted, *NGN3*-mCherry^{low}, or *NGN3*-mCherry^{high} cells with *INS*-Venus. Scale bars = 100 μm. *EP*, endocrine progenitor.

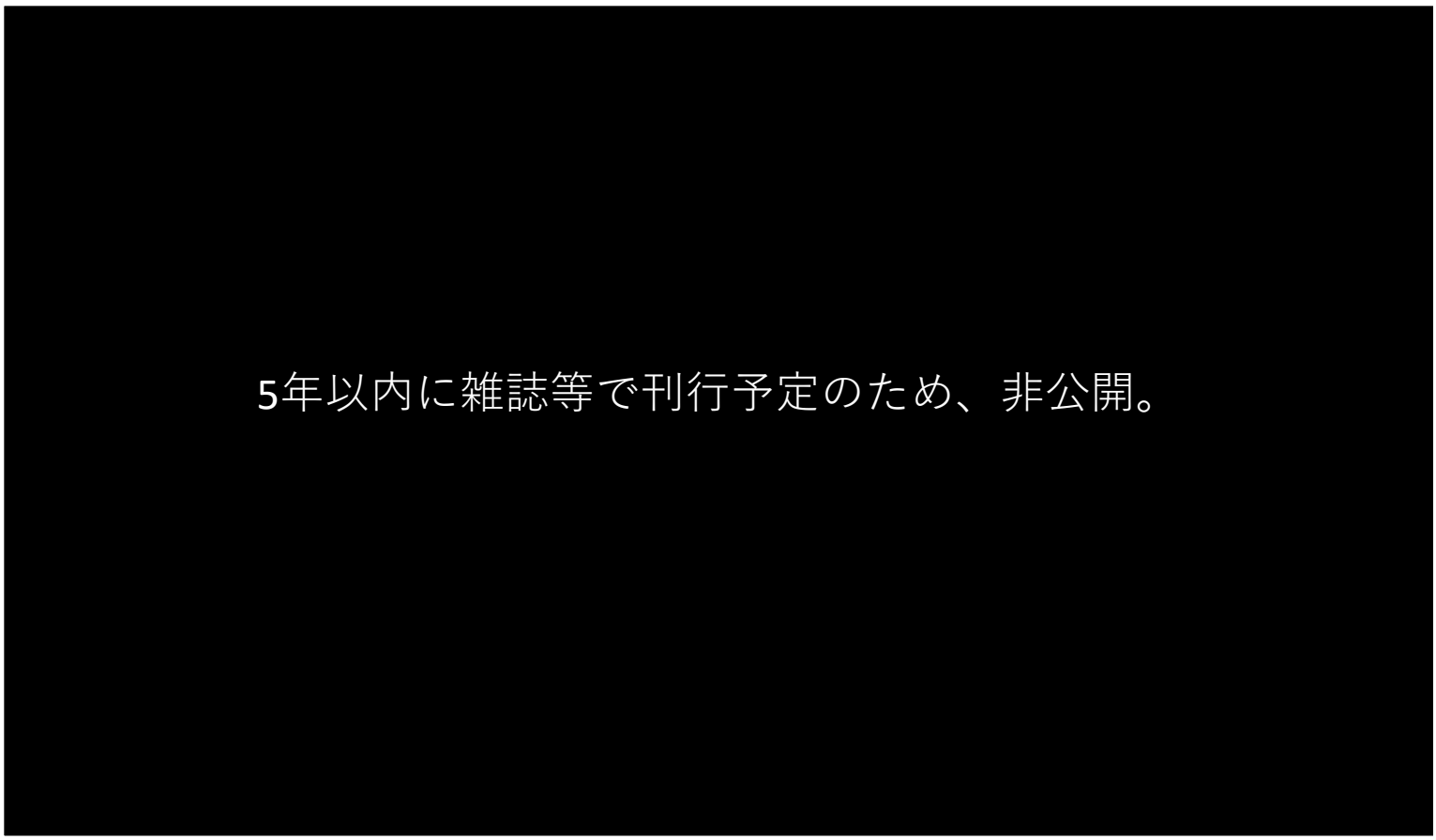

Figure 9. Expression analysis of endocrine markers

mRNA expression was analyzed by qRT-PCR and shown are the relative expression levels of the endocrine marker gene *INS* (insulin), *GCG* (glucagon), and *SST* (somatostatin), in pre-sorted, *NGN3*-mCherry^{low}, and *NGN3*-mCherry^{high} cells. Expression level of each gene is shown as relative expression level of pre-sorted sample as 1.0. Error bar represents the mean + SD of 3 independent experiments. Statistical analysis was performed using the Turkey-Kramer test. *, significantly different from each of the other two fractions. *$P < 0.05$.

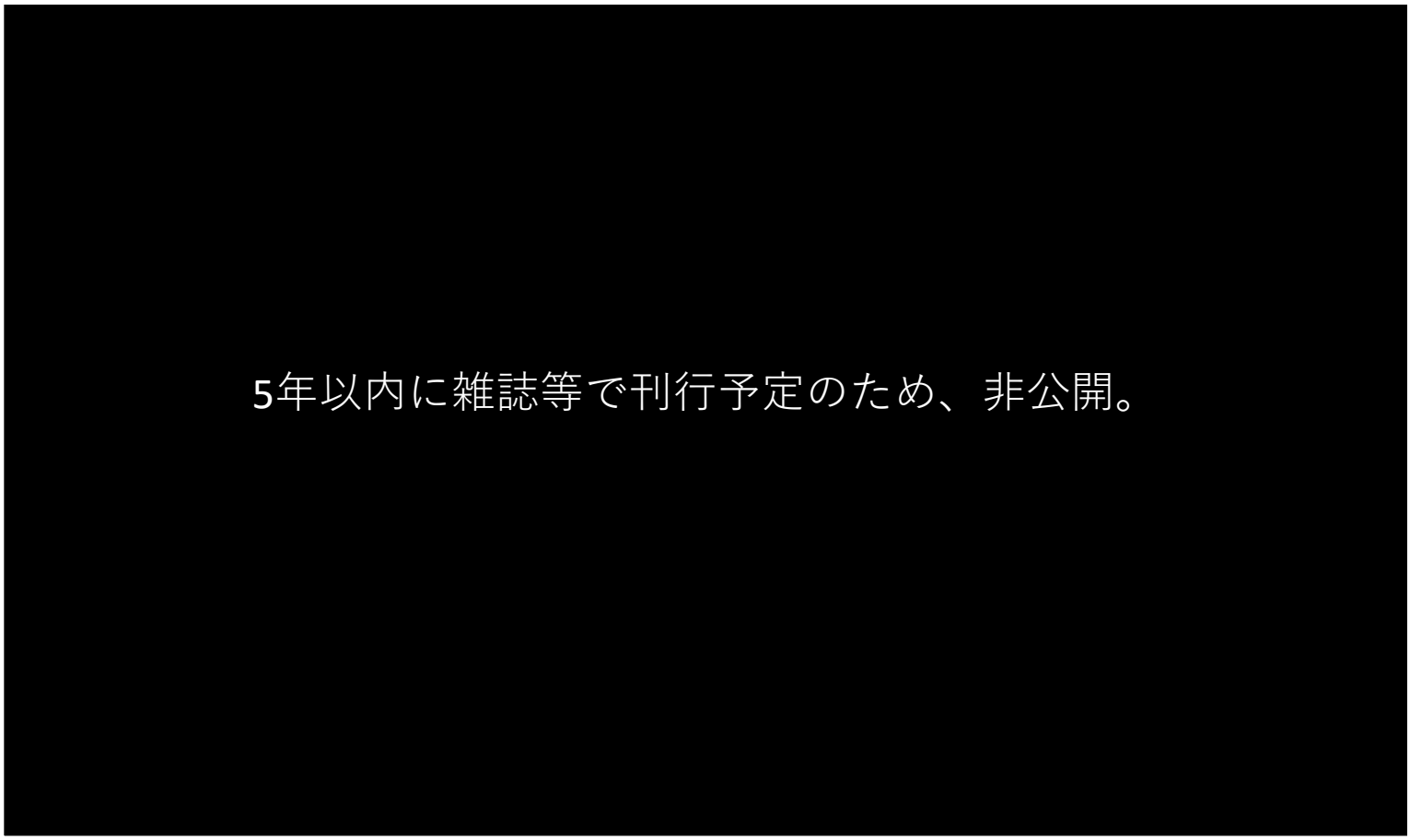

Figure 10. Expression of endocrine markers in islets derived from hiPSCs

Immunofluorescent staining of spheroids from pre-sorted, *NGN3*-mCherry^{low}, or *NGN3*-mCherry^{high} cells was performed with antibodies recognizing insulin precursor C-peptide (C-pep, green), glucagon (GCG, red), and somatostatin (SST, blue), together with nuclear staining (white) using 4'-6- diamidino-2-phenylindole (DAPI). Scale bars = 50μm.

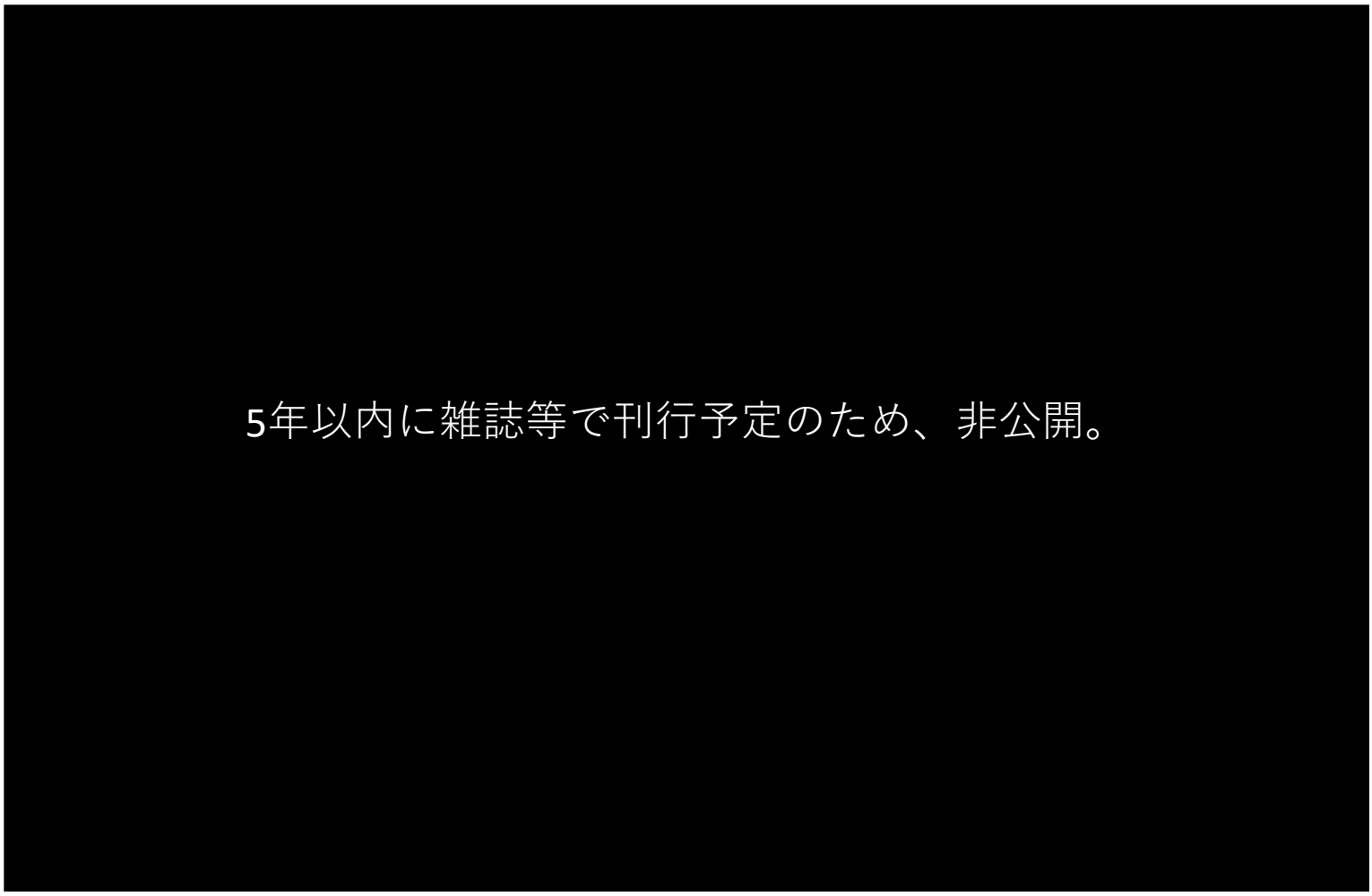

Figure 11. Insulin secretion from hiPSC-derived islets

Glucose-stimulated insulin secretion (GSIS) of pancreatic islets derived from pre-sorted, *NGN3*-mCherry^{low} cells, or *NGN3*-mCherry^{high} cells. C-peptides secreted in supernatant of culture with indicated glucose concentrations for 1 hour were determined. The y-axis shows total secreted C-peptide normalized to cell numbers. Left graph represents average of the 3 independent experiments. Error bar represents the mean + SD of 3 independent experiments. Right graph represent the secretion of each lot.

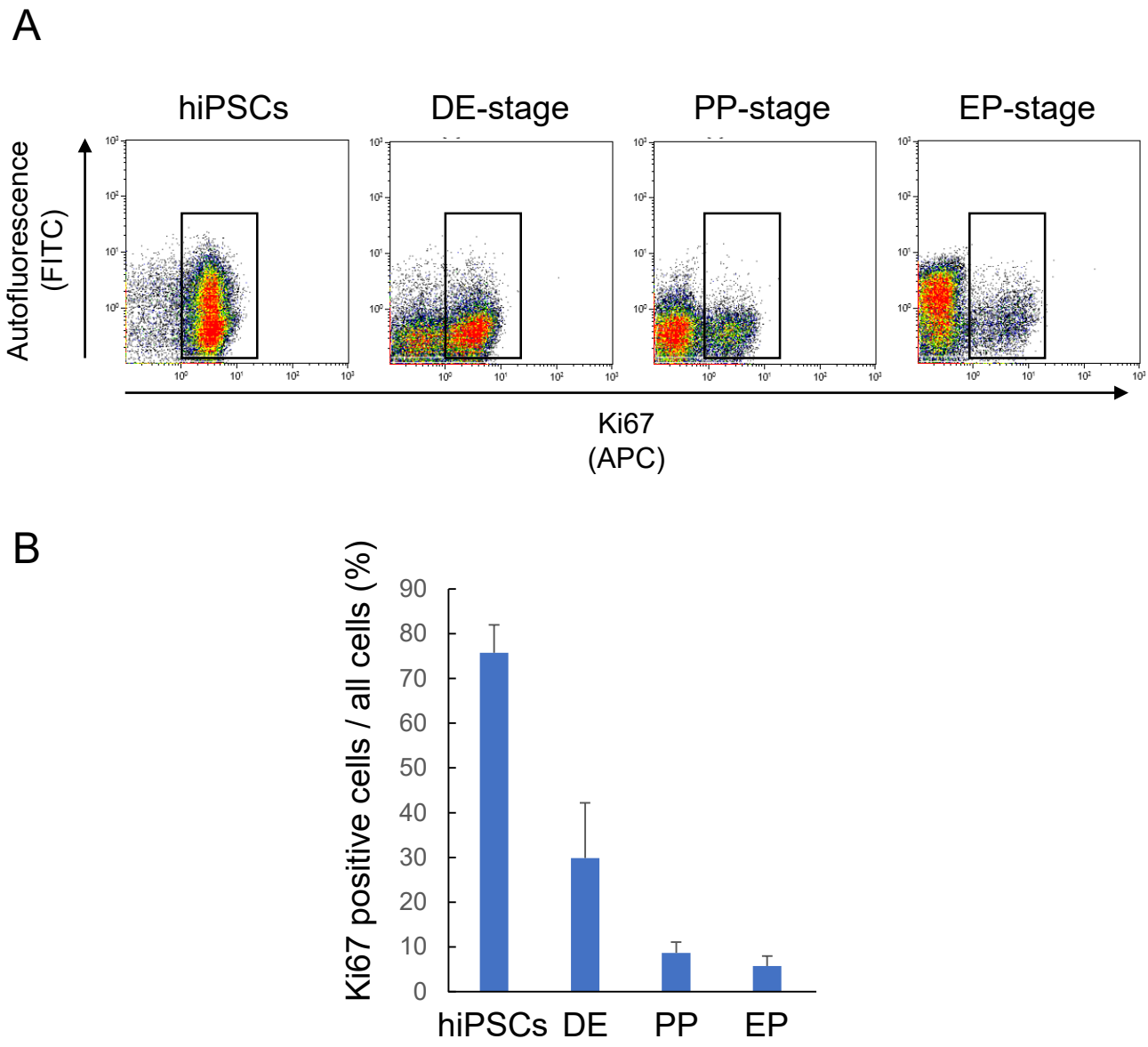

Figure 12. Expression of Ki67, a cell proliferation marker, by flow cytometry analysis in each stage

(A) Flow cytometry analysis of Ki67 expression in stepwise differentiation from hiPSCs to EP-stage cells. (B) The percentage of cells positive for Ki67 in stepwise differentiation from hiPSCs to EP-stage cells. Error bar represents the mean + SD of 4 independent experiments. *hiPSCs*, human induced pluripotent stem cells; *DE*, definitive endoderm; *PFG*, posterior foregut; *PP*, pancreatic progenitor; *EP*, endocrine progenitor.

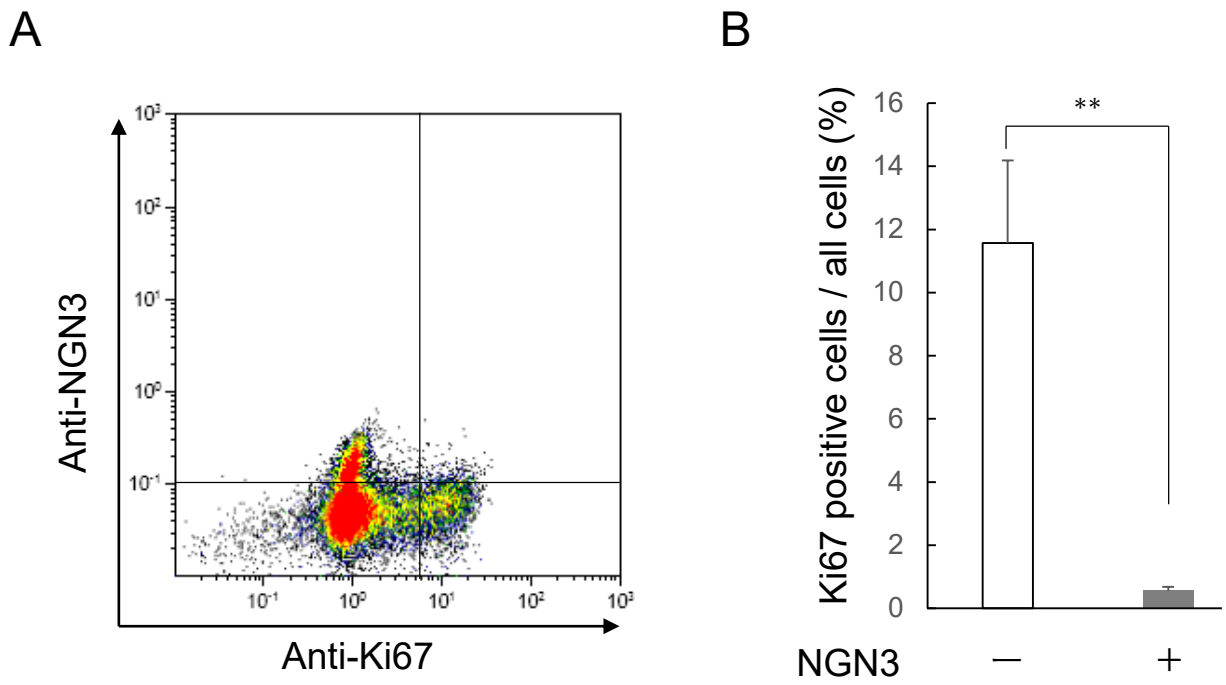

Figure 13. Expression of Ki67 in EP-stage cells

(A) Flow cytometry analysis of NGN3 and Ki67 in EP-stage cells. (B) A comparison of the percentage of Ki67 positive cells in NGN3(-) and NGN3(+). Error bar represents the mean + SD of five independent experiments. Statistical analysis was performed using the Mann-Whitney U test. **$P < 0.01$.

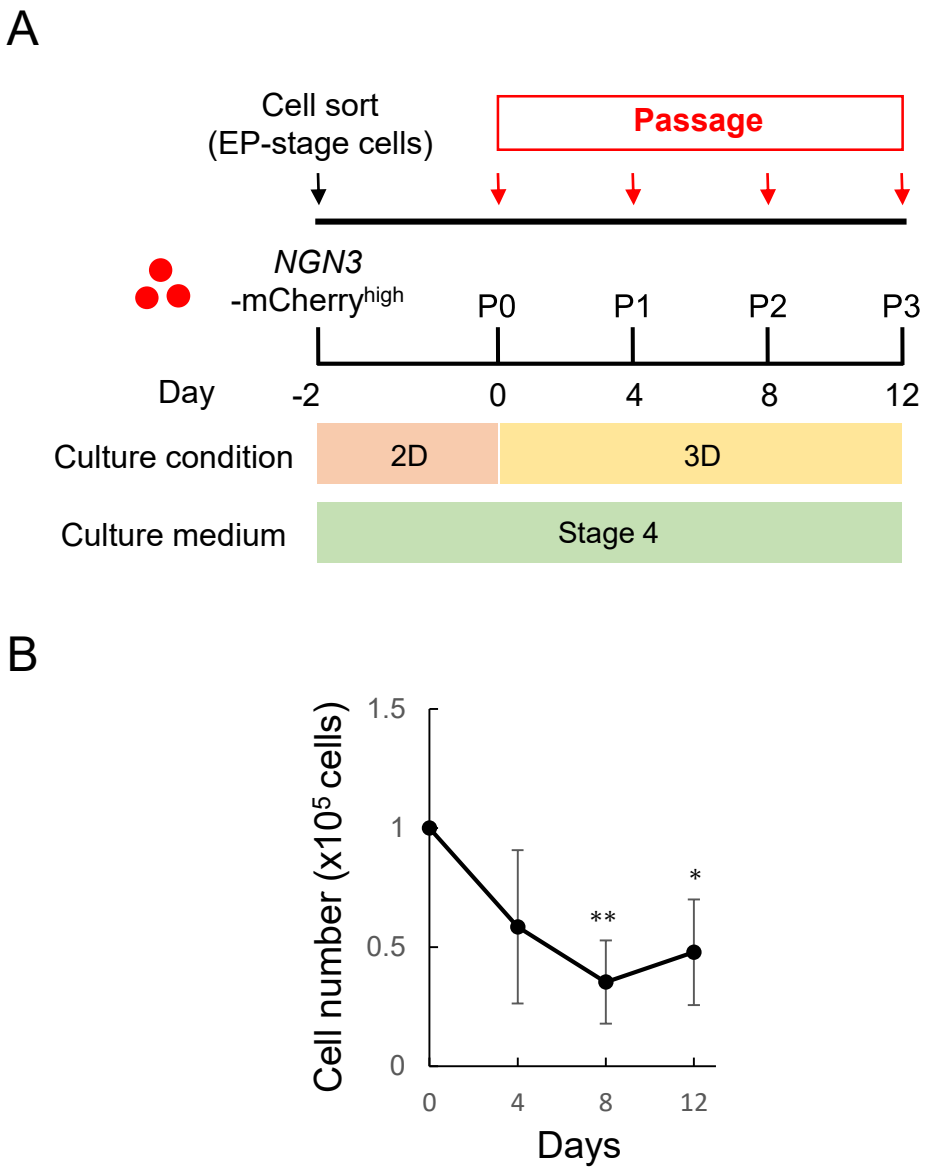

Figure 14. Cell growth arrest of *NGN3*-mCherry^{high} cells

(A) Schematic image of culture methods of *NGN3*-mcherry^{high} cells for 12 days. *NGN3*-mCherry^{high} cells were sorted from EP-stage cells, cultured for 2 days on 2 dimensional (2D) culture in Stage 4 medium, and passaged every 4 days on 3 dimensional (3D) cultured in Stage 4 medium. (B) Growth curve of *NGN3*-mCherry^{high} cells for 12 days. Error bar represents the mean ± SD of 4 independent experiments. Statistical analysis was performed using the Mann-Whitney U test. * and **, significantly different from day 0. *$P < 0.05$, ** $P < 0.01$.

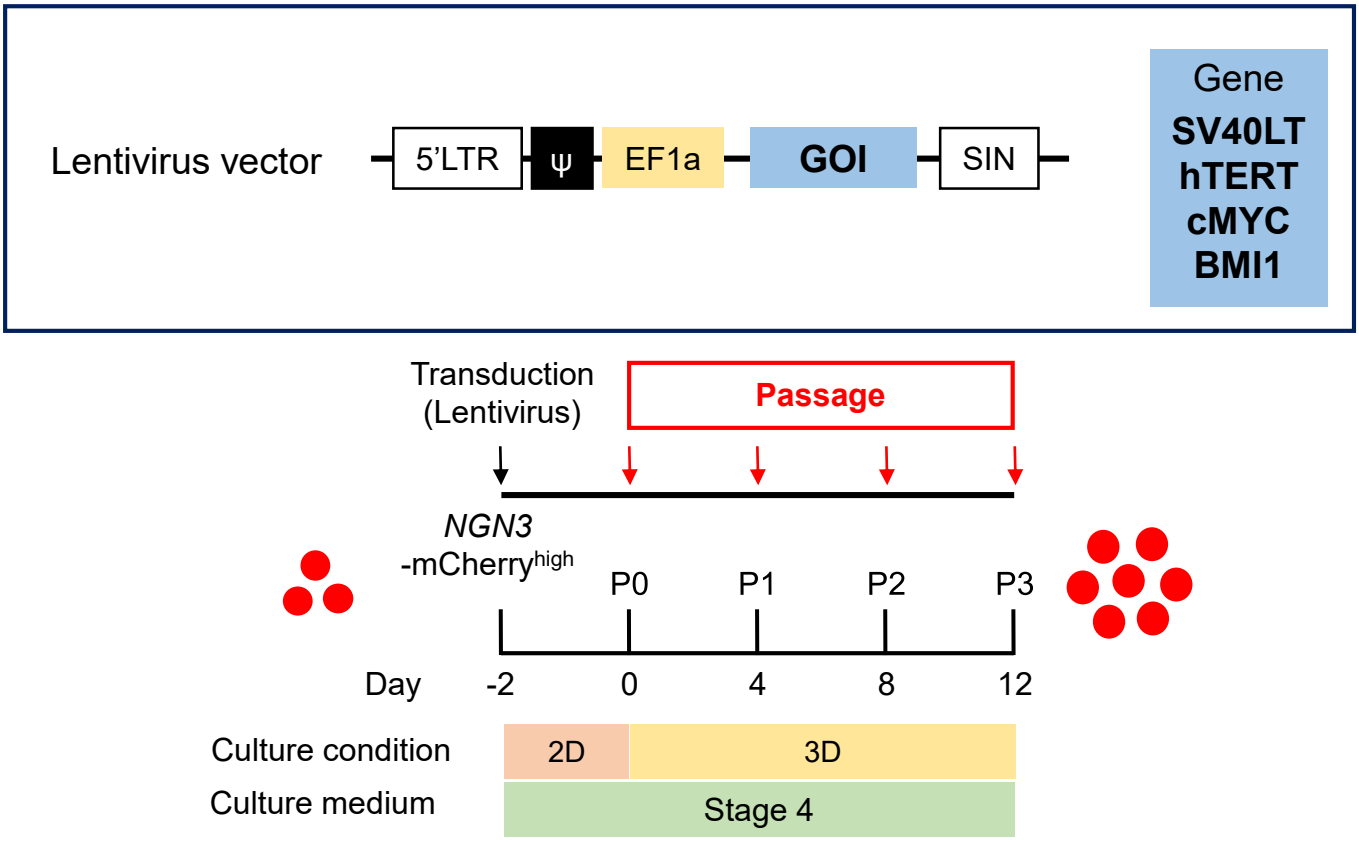

Figure 15. Structure of lentivirus vector and culture methods for the expansion of *NGN3*-mCherry^{high} cells

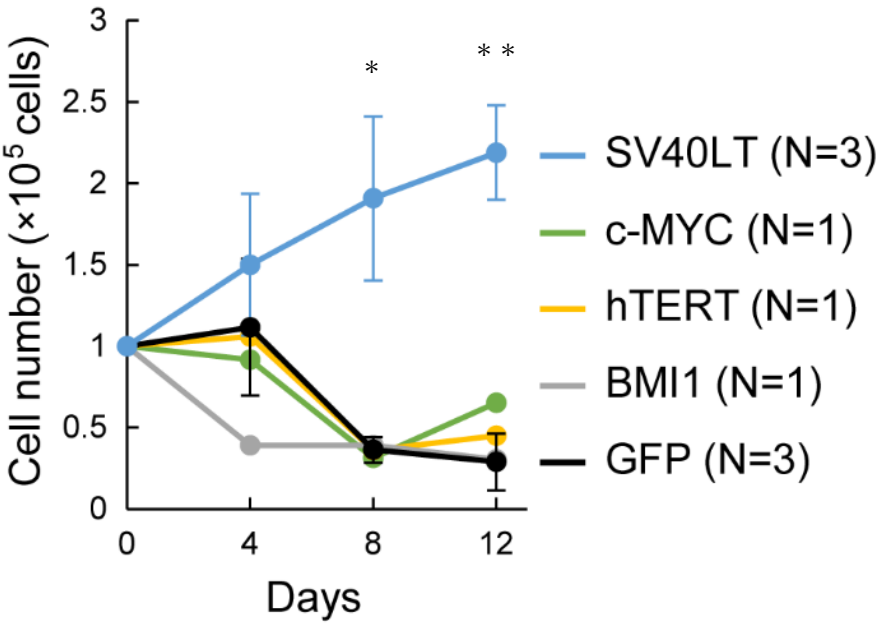

Figure 16. Growth curve of *NGN3*-mCherry^{high} cells expressing growth-promoting genes by lentivirus

Error bar represents the mean ± SD of three independent experiments (SV40LT and GFP (negative control)) and a single experiment (c-MYC, hTERT, and BMI1). Statistical analysis was performed using the Student's t test. * and **, significantly different from SV40LT of day 0. *P < 0.05, ** P < 0.01.

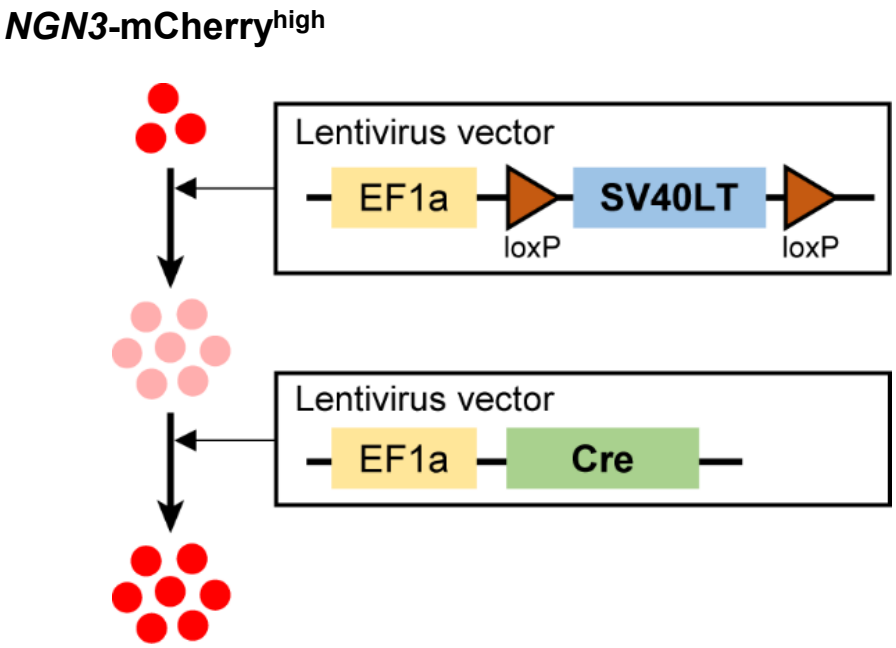

Figure 17. Induction and removal of SV40LT expression in *NGN3*-mCherry^{high} cells by using SV40LT-loxP and LV-Cre lentivirus vectors

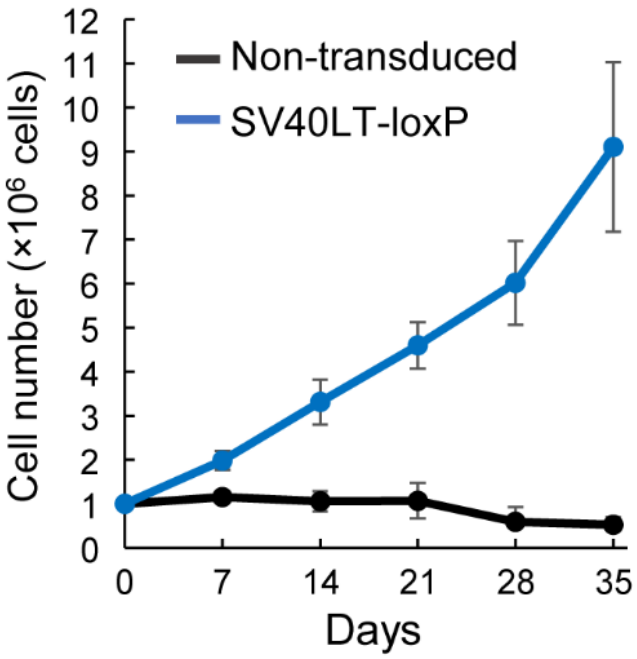

Figure 18. Growth curve of *NGN3*-mCherry^{high} cells expressing SV40LT genes by lentivirus

Blue line denotes cells transduced with SV40LT-loxP, and the black line denotes these without transduction. Error bar represents the mean ± SD of five independent experiments.

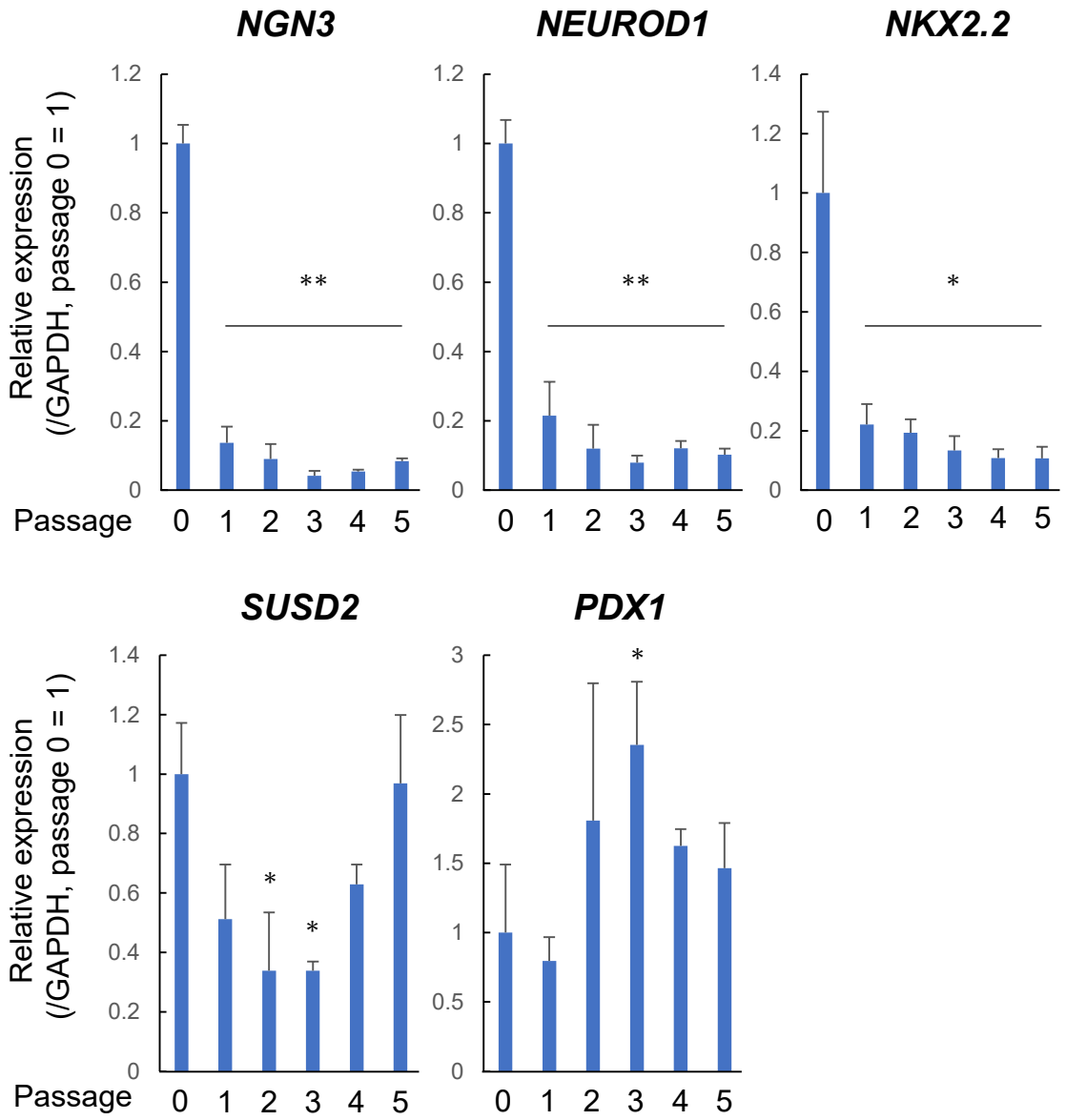

Figure 19. Expression of EP markers in expanded *NGN3*-mCherry^{high} cells

qRT-PCR analysis of endocrine progenitor markers (*NGN3*, *NEUROD1*, and *NKX2.2*) and an endocrine progenitor surface marker *SUSD2* and a pancreatic progenitor marker *PDX1* in expanded *NGN3*-mCherry^{high} cells during five passages. Expression level of each gene is shown relative expression level of averaged passage 0 samples as 1.0. Error bar represents the mean + SD of 3 independent experiments. Statistical analysis was performed using the Student's t test. * and **, significantly different from passage 0. *P < 0.05, ** P < 0.01.

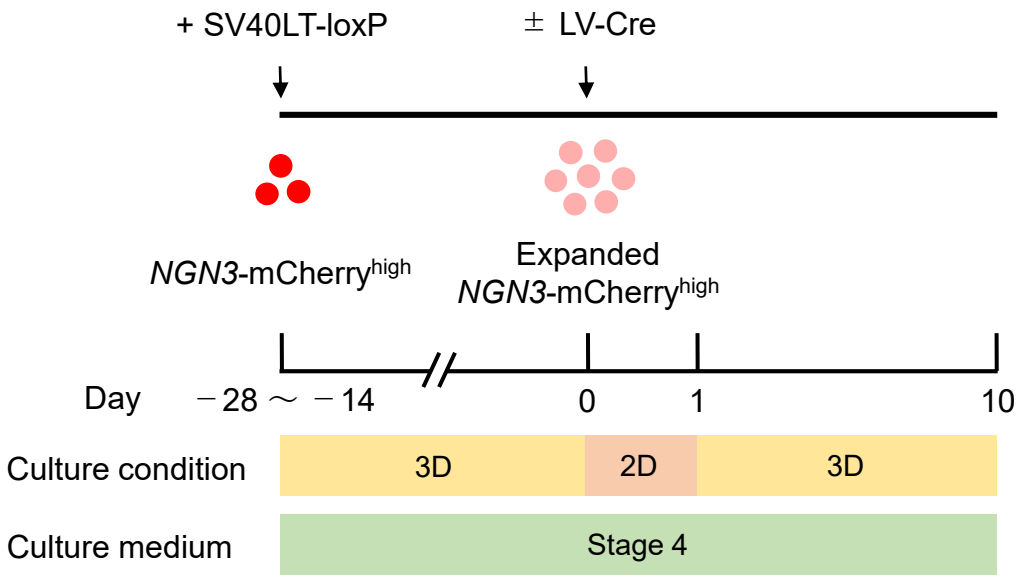

Figure 20. Schematic image of culture method of expanded *NGN3*-mcherry^{high} cells treated with or without LV-Cre.

After expansion of *NGN3*-mCherry^{high} cells, cultured for 1 day on 2D culture in Stage 4 medium to transduce LV-Cre, and cultured 9 days on 3D cultured in Stage 4 medium.

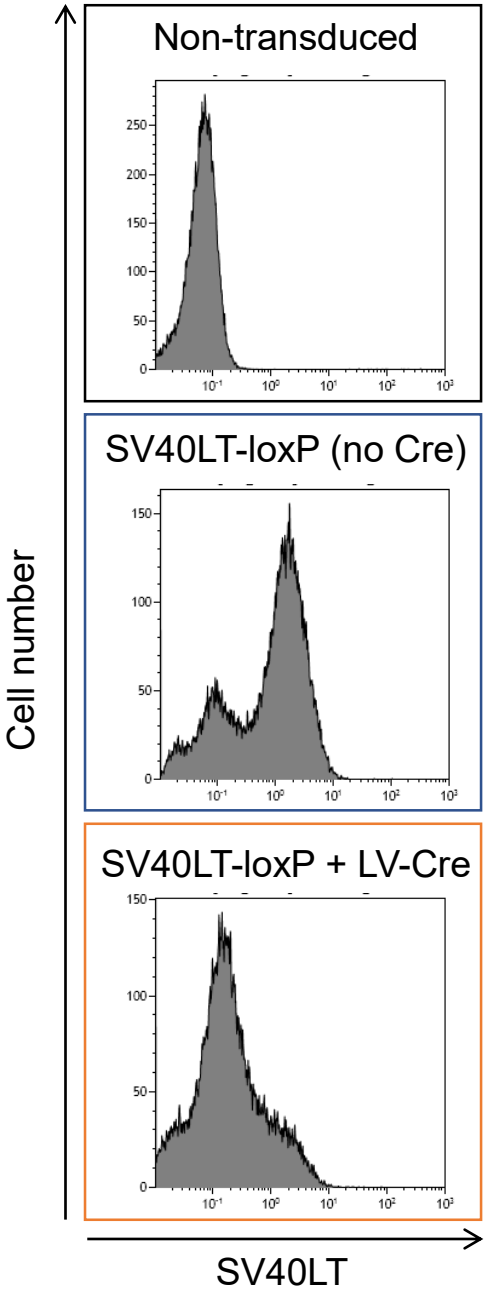

Figure 21. Expression of SV40LT estimated by flow cytometric analysis

Flow cytometric analysis of SV40LT expression with or without LV-Cre induction shown by histogram plotting. Black box indicates negative control experiments (Non-transduced of lentivirus in *NGN3*-mCherry^{high} cells), blue box and orange box indicate transduced without or with LV-Cre, respectively.

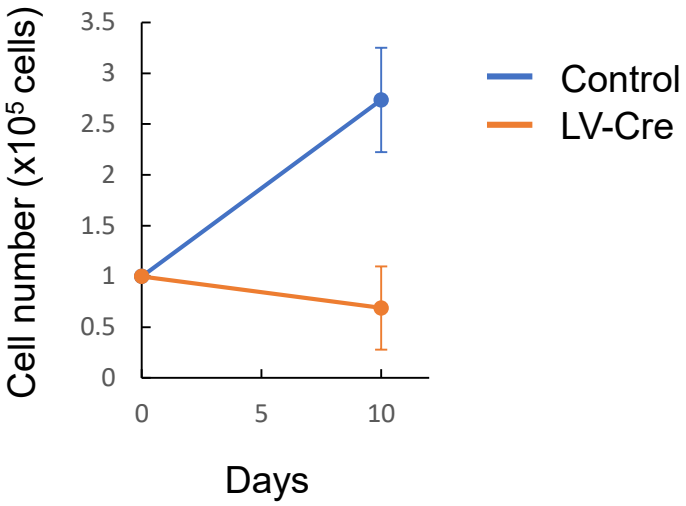

Figure 22. Growth curve of *NGN3*-mCherry^{high} cells treated with or without LV-Cre

Orange line donates transduced with LV-Cre, and blue line denotes without lentivirus transduction (Control). Error bar represents the mean ± SD of three independent experiments.

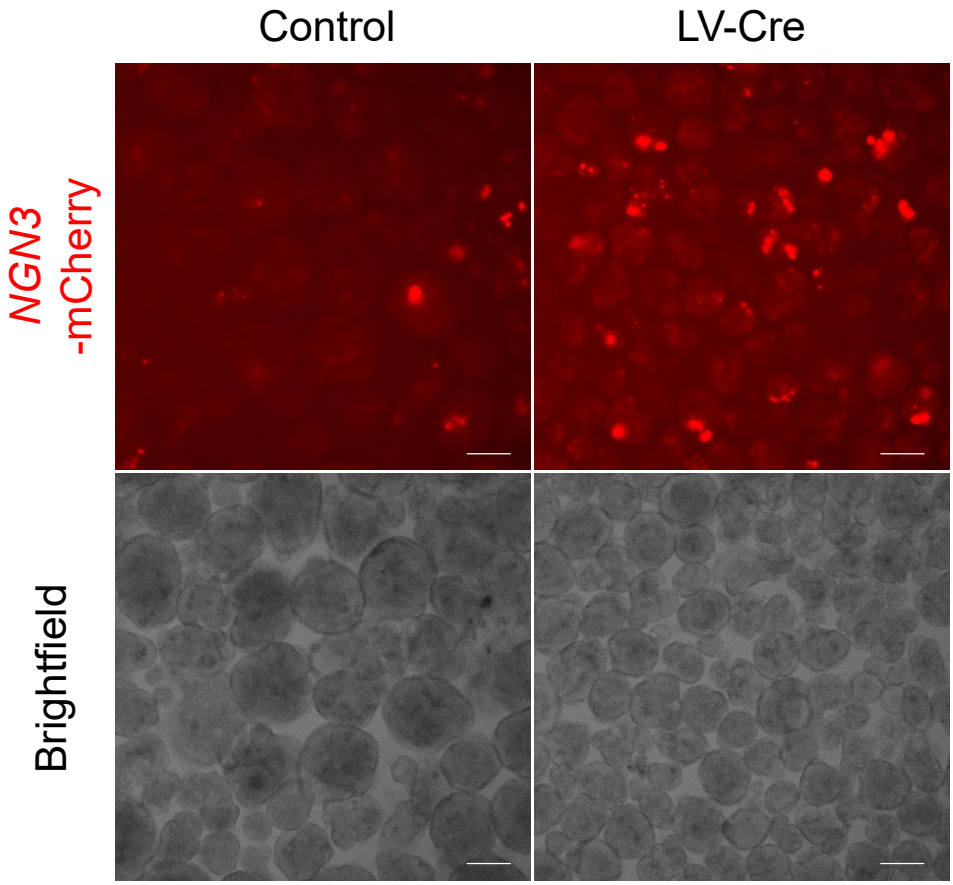

Figure 23. Representative images of *NGN3*-mCherry^{high} cells treated with or without LV-Cre

The live cell picture on day 10 in suspension culture after transduced with or without LV-Cre. Upper, mCherry fluorescence; lower, brightfield. Scale bars, 100 μm.

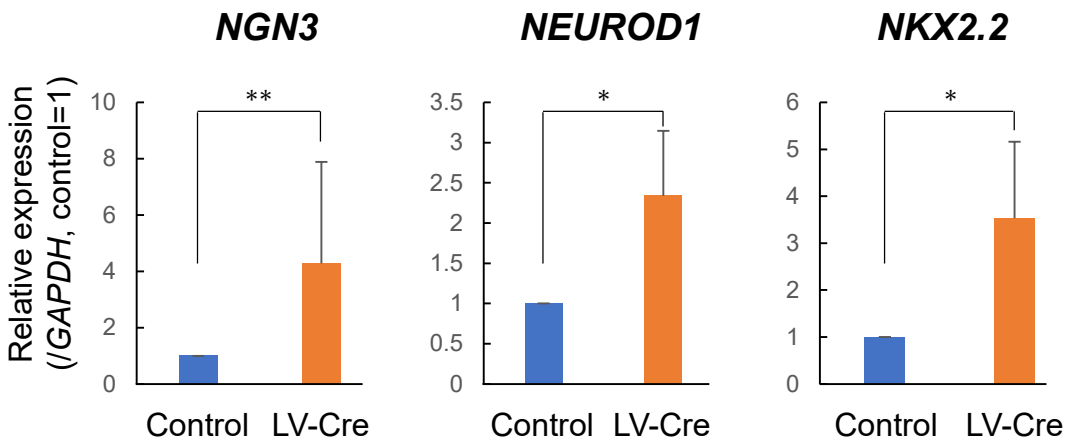

Figure 24. Transduction of LV-Cre rescues expression of endocrine-lineage commitment genes in *NGN3*-mCherry^{high} cells

qRT-PCR analysis of endocrine progenitor markers *NGN3*, *NEUROD1*, and *NKX2.2* in *NGN3*-mCherry^{high} cells transduced with LV-Cre compared with the cells without Cre. Expression level of each gene is shown relative expression levels of averaged control sample as 1.0. Error bar represents the mean + SD of five independent experiments. Statistical analysis was performed using the Mann-Whitney U test. *P < 0.05, **P < 0.01.

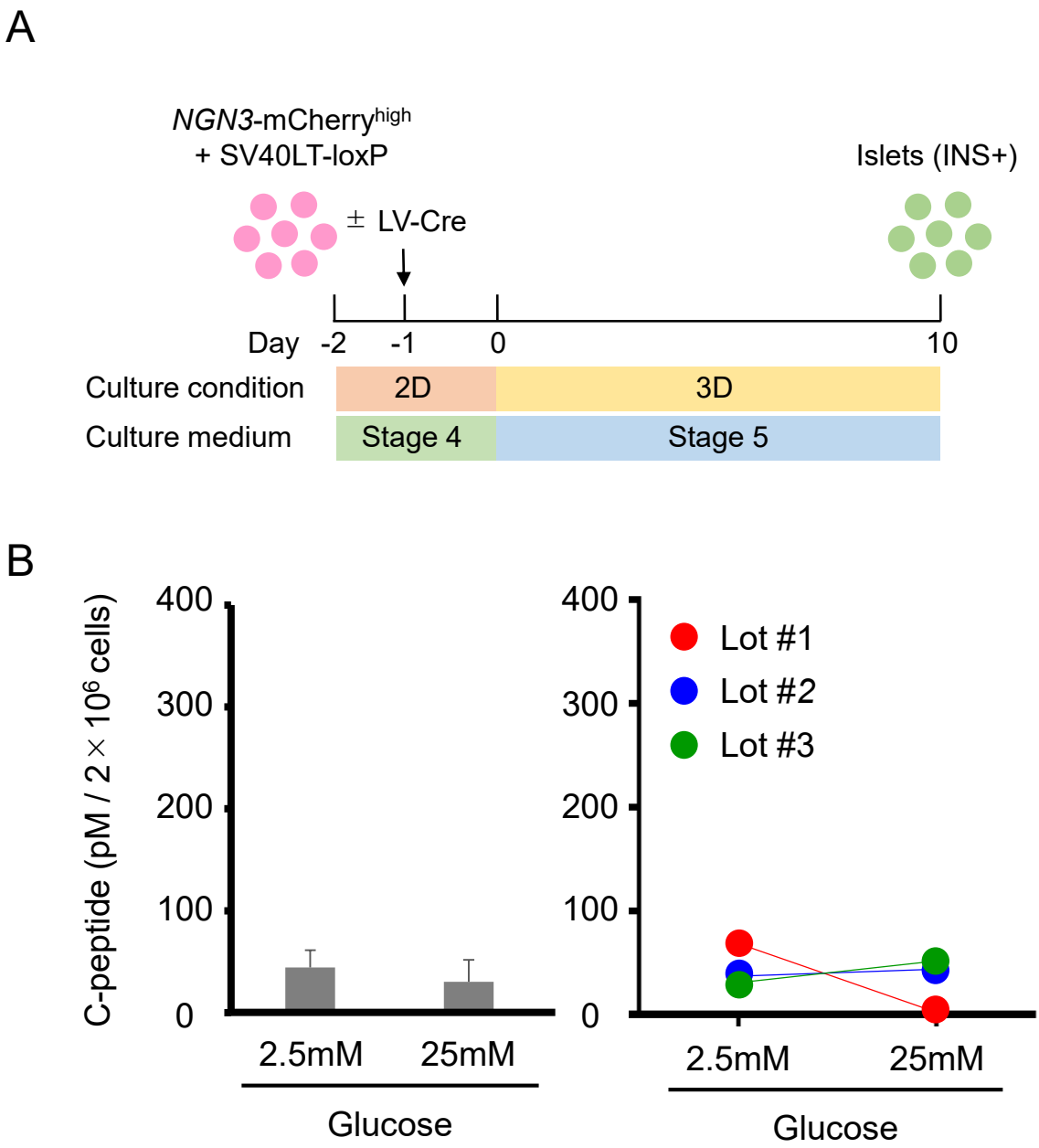

Figure 25. Pancreatic islet differentiation from *NGN3*-mCherry^{high} cells immediately after LV-Cre transduction

(A) Schematic differentiation into hiPSC-derived islets from expanded *NGN3*-mCherry^{high} cells immediately after LV-Cre transduction. (B) Glucose challenge test; islets derived from expanded *NGN3*-mCherry^{high} cells immediately after LV-Cre infection were cultured in the presence of indicated glucose concentrations for 1 hour and the amounts of C-peptide in the supernatant were examined. The y-axis shows total secreted C-peptide normalized by cell numbers. Left graph represents average of the 3 independent experiments. Error bar represents the mean + SD of 3 independent experiments. Right graph represent the secretion of each lot.

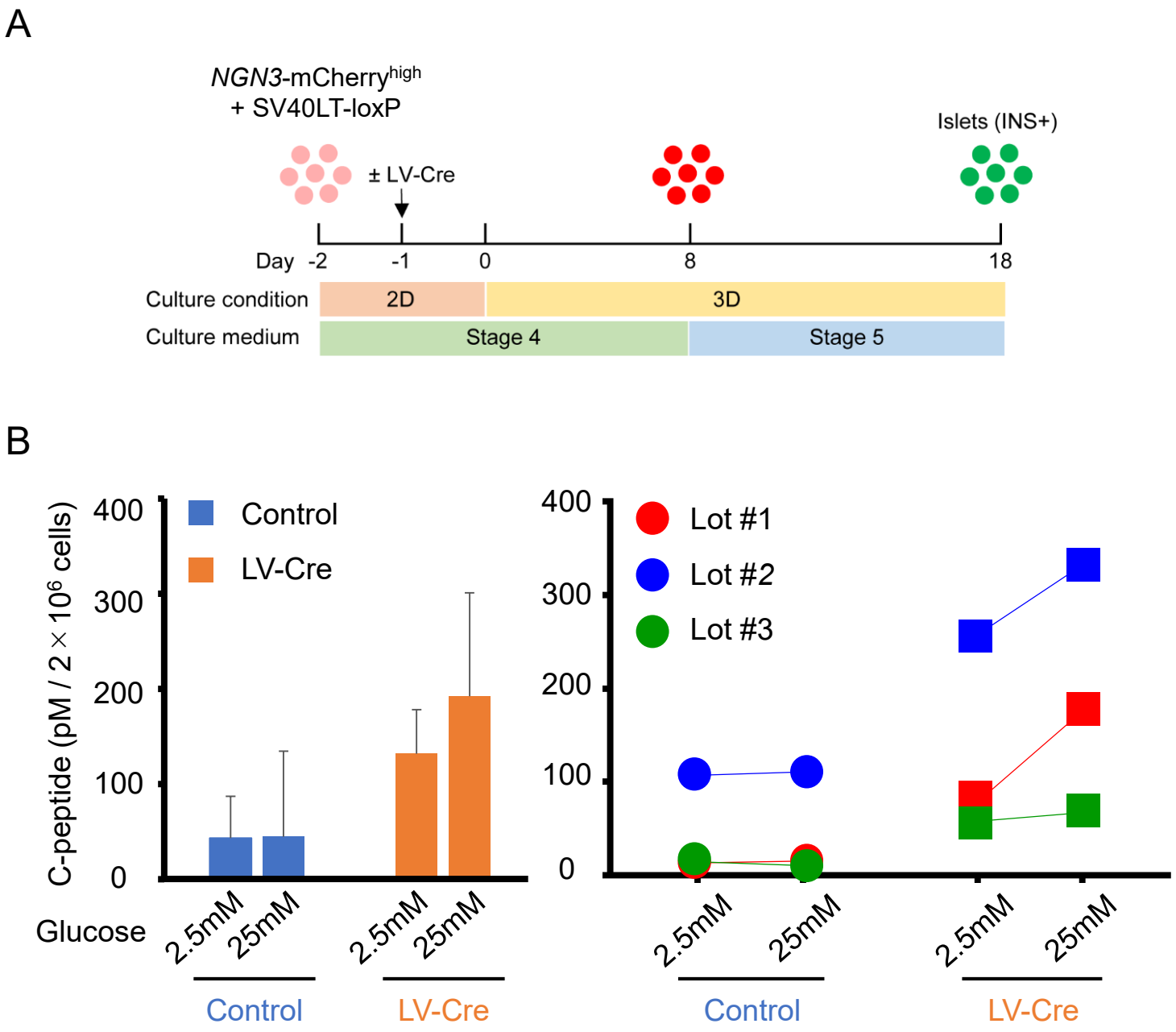

Figure 26. Differentiation into pancreatic islets from expanded *NGN3*-mCherry^{high} cells

(A) Schematic image of differentiation into hiPSC-derived islets from expanded *NGN3*-mCherry^{high} cells with or without LV-Cre. (B) Glucose challenge test; islets derived from expanded *NGN3*-mCherry^{high} cells with or without transduction with LV-Cre were cultured using indicated glucose concentrations for 1 hour and the amounts of C-peptide in the supernatant were examined. The y-axis shows total secreted C-peptide normalized by cell numbers. Left graph represents average of the 3 independent experiments. Error bar represents the mean + SD of 3 independent experiments. Right graph represent the secretion of each lot.

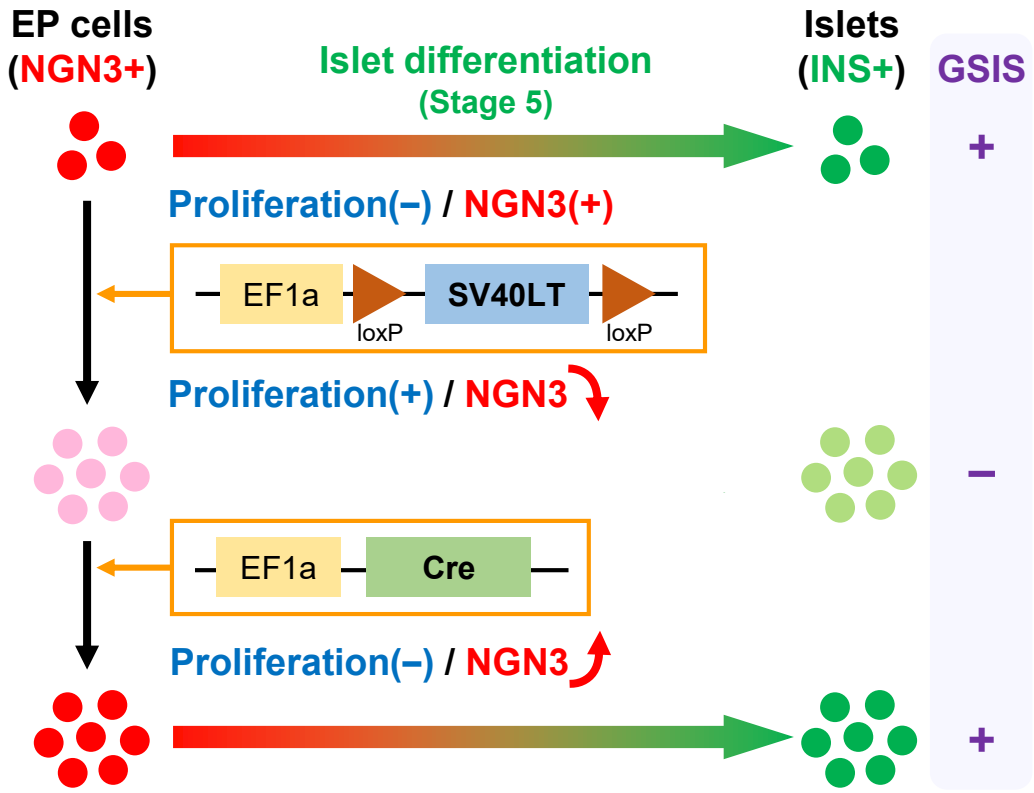

Figure 27. Summary of endocrine progenitor cell proliferation and pancreatic islet differentiation

Table 1: Primary antibodies used for immunocytofluorescence and flow cytometry

Antibody	Host	Source	Dilution
C-peptide	Mouse	05-1109, Millipore	1:100
Glucagon	Rabbit	A0565, Dako	1:500
Somatostatin	Goat	sc7819, Santa Cruz Biotechnology	1:100
Neurogenin3	Mouse	F25A1B3-S, DSHB	1:100
Ki67	Rat	14-5698-82, eBioscience	1:400
SV40LT	Mouse	sc-147, Santa Cruz Biotechnology	1:50
CD184 (CXCR4)	Mouse	306510, Biolegend	1:400
CD117 (c-Kit)	Mouse	313212, Biolegend	1:400
Pdx1	Goat	AF2419, R&D System	1:50

Table 2: Secondary antibodies used for immunocytofluorescence and flow cytometry

Conjugate	Host	Source	Dilution
Alexa Fluor 488	Rabbit	A21206, lifetechnologies	1:500
Alexa Fluor 555	Goat	A21432, lifetechnologies	1:500
Alexa Fluor 555	Mouse	A21424, lifetechnologies	1:500
Alexa Fluor 647	Rat	A21247, lifetechnologies	1:500
Alexa Fluor 647	Goat	A21447, lifetechnologies	1:500
Alexa Fluor 647	Mouse	A31571, lifetechnologies	1:500
Alexa Fluor Plus 647	Mouse	A32728, Invitrogen	1:300

Table 3: Primer sequences for qRT-PCR

Gene Symbol	Forward Primer	Reverse Primer
GAPDH	AGCCACATCGCTCAGACAC	GCCCAATACGACCAAATCC
NEUROG3	GCTCATCGCTCTCTATTCTTTTGC	GGTTGAGGCGTCATCCTTTCT
NEUROD1	GTTCTCAGGACGAGGAGCAC	CTTGGGCTTTTGATCGTCAT
NKX2.2	GGCCTTCAGTACTCCCTGCA	GGGACTTGGAGCTTGAGTCCT
SUSD2	GGCACCGCCAACACCTCA	GCGTGGGCAGCGACTTGA
PDX1	AAGTCTACCAAAGCTCACGCG	GTAGGCGCCGCCTGC
PAX6	ATTCTGCAGGTGTCCAACGG	CACTCCCGCTTATACTGGGC
GCG	GCTGCCAAGGAATTCATTGC	CTTCAACAATGGCGACCTCTTC
SST	ACCCCAGACTCCGTCAGTTT	ACAGCAGCTCTGCCAAGAAG

Acknowledgments

I would like to thank my supervisor, Prof. Atsushi Miyajima, Drs. Ami Watanabe and Yasuhiro Nakano, and Prof. Tatsuo Michiue for the thoughtful mentoring. I also would like to thank Ms. Chizuko Koga, Yoshiko Kamiya, and Naoko Miyata for their skillful assistance and the member of the Miyajima lab for helpful discussion and advice. Lastly, I appreciate my family who have supported me at any time.